D 63612

Vol. 2 Number 7

August 25, 2005

PLASMA PROCESSES AND POLYMERS

www.plasma-polymers.org

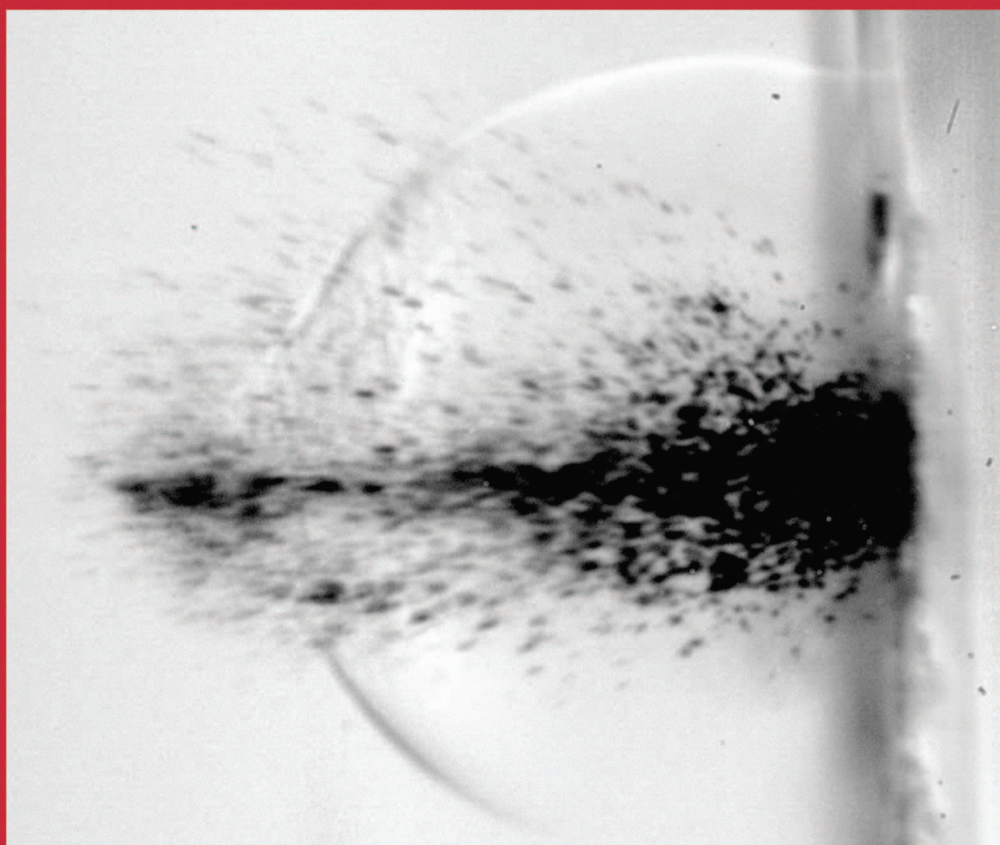

Editors-in-Chief
Riccardo d'Agostino, Bari
Pietro Favia, Bari
Christian Oehr, Stuttgart
Michael R. Wertheimer, Montreal

Manuscript Submission & Personal Homepage
manuscriptXpress
http://www.manuscriptXpress.com

ISSN 1612-8850 Plasma, 2, No. 7, 517 – 596 (2005)

Summary: This work reviews the interaction of photons with polymers with an emphasis on UV laser ablation and surface modification using VUV lamps. Laser ablation of polymers is an established process in industrial applications, but the mechanisms of ablation are still controversial. Different polymers, such as poly(methyl methacrylate), polyimides and specially designed polymers are used as examples to show that the mechanism is a mixture of photochemical and photothermal features which are closely related to the polymer structure and properties. Different approaches to probe the ablation mechanisms and to improve ablation are discussed. Photoactive groups have been introduced into the polymer structure to improve the quality of ablation and to elucidate the ablation mechanisms. The experimental techniques to probe the ablation mechanism range from time-resolved measurements, such as shadowgraphy, ToF-MS, and ns-surface interferometry to variations of the irradiation wavelengths and pulse lengths. The necessity for a critical evaluation of the experimental procedures and analysis is discussed exemplary for polyimides. The data for different types of polyimides are mixed up and some experimental procedures are possibly causing problems for the data evaluation. Various recent trends for laser ablation, such as ultrafast ablation or VUV ablation are also discussed. Surface modifications of polymers using VUV photons from lamps are discussed for oxidation and nitriding of poly dimethylsiloxane (PDMS) and polyolefines. The mechanism of the PDMS surface oxidation is presented in detail.

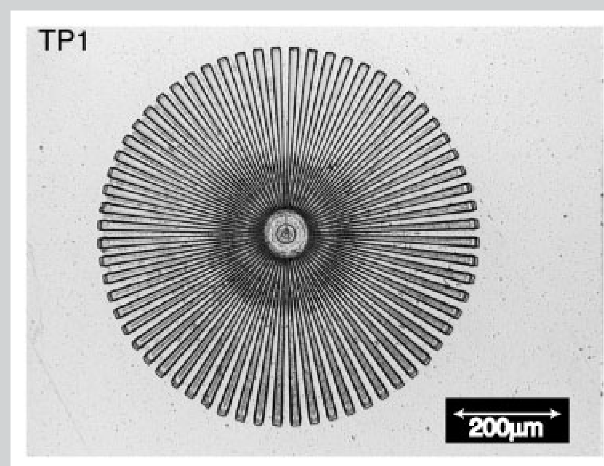

Ablation pattern in TP1 created by 308 nm irradiation using a gray tone phase mask.

Interaction of Photons with Polymers: From Surface Modification to Ablation

Thomas Lippert

Paul Scherrer Institut, 5232 Villigen PSI, Switzerland
E-mail: thomas.lippert@psi.ch

Received: April 1, 2005; Revised: June 14, 2005; Accepted: June 17, 2005; DOI: 10.1002/ppap.200500036

Keywords: laser ablation; polymer treatments; surface modification; VUV irradiation

Introduction

The interaction of photons with a polymer can result in a large variety of reactions which range from the modification of the polymer surface to the complete decomposition. The latter normally results in ablation and/or carbonization of the irradiated polymer area. The first reports about laser ablation of polymers were published in 1982[1,2] and since then numerous studies dealing with ablation of a wide variety of polymers and the ablation mechanism(s) have been published as well as are well summarized in various reviews.[3–8] Discussion relating to the ablation mechanism started very soon after the discovery of ablation, and up to now no general agreement exists whether the mechanism is photochemical or photothermal. Recent papers[9] and reviews[10] favor a photothermal mechanism, but these studies are based on modeling of data for one polymer, i.e., Kapton™. This approach may be reasonable, but we should also not forget that there exists a long standing research topic, i.e., organic polymer photochemistry,[11] that has proven that irradiation of organic molecules or polymers with UV photons leads to in photochemical reactions. Therefore, it is also very likely that under ablation conditions, i.e., much higher fluences, photochemical reactions take place. The ablation products and the products of these photochemical reactions are related to the type of polymer and irradiation wavelength. Polymers may be classified for photon-induced reactions into polymers that

DOI: 10.1002/ppap.200500036
© 2005 WILEY-VCH Verlag GmbH & Co. KGaA, Weinheim

can depolymerize upon irradiation and into polymers that decompose into fragments. The assignment of polymers into one of these two classes is closely related to the synthesis of the polymer: polymers that are formed by radical polymerization from monomers which contain double bonds are classical candidates for depolymerization upon irradiation, while polymers that are formed by reactions such as polycondensation will not decompose into the monomers upon irradiation. This means of course that no films with the same chemical structure and/or molecular weight can be obtained by pulsed laser deposition from these polymers as targets. A possible exception may be a process termed resonant infrared pulsed laser deposition (RIR-PLD)[12] where a tunable IR laser, i.e., a free electron laser (FEL), is applied as irradiation source. Other processes, such as matrix-assisted pulsed laser evaporation (MAPLE)[13] or RIR-MAPLE[14] may be utilized to form polymer films with intact structures of the films and without any pronounced degradation of the polymer. All above-mentioned photon-induced polymer processing methods, i.e., ablation/structuring, surface modification, and film deposition are either already applied in applications or are under development. The most prominent examples may be the via-hole drilling in multichip modules at IBM[15] or the nozzle drilling for inkjet printer.[16] For both processes laser ablation with UV lasers is applied, while the polymers are typically polyimides or polyamides. In this article two of these processes, i.e., laser ablation and surface modification, are discussed in more detail, with an emphasis on the chemistry, possibilities of designed polymers, and mechanisms behind these processes.

Discussion

Classification of Polymers for Laser Ablation

A typical example for a polymer that can depolymerize at least partly, i.e., reversibly forming the monomer, is poly(methyl methacrylate) (PMMA) (see Figure 1), while typical examples for polymers that decompose into new fragments are polycarbonates (Figure 2) and polyimides (chemical structures and monomers are shown in Figure 3). It is obvious from the monomers and the reactions to synthesize the polymers, i.e., the elimination of HCl or H_2O, that these polymers will decompose upon photon irradiation into some fragments that cannot be identical with the monomers.

In the case of PMMA, decomposition into the monomer is possible, but a complete transformation into monomers is only possible for a pure thermal degradation at temperatures above the ceiling temperature T_C (104 °C) of PMMA. T_C is defined as the temperature where the equilibrium between polymer and monomer is totally on the side of the monomer. The analysis of the ablation products upon irradiation with UV light, however, reveals that only a small amount, i.e., ≈1% for irradiation at 248 nm and ≈18% at 193 nm[17,18] of the products is in fact the monomer. The detected products are at least partially compatible with the well-known products of the photolysis of PMMA (shown in Figure 4). The photodecomposition starts with the excitation of the monomer unit, where for a 248 nm irradiation the $n \rightarrow \pi^*$ transition of the ester group is excited. The following steps are the side chain scission of the ester group (shown in Figure 4, step 1) which is followed by hydrogen abstraction by the radicals, and elimination of CO or CO_2 (step 2 in Figure 4). The initial reaction, i.e., the bond scission next to the carbonyl group is one of the most prominent photochemical reactions, known as Norrish type I reaction or α-cleavage. The successive steps are the main chain scission that is accompanied by the creation of double bonds (chain end and mid chain) which is also detected during UV laser irradiation of PMMA.[19]

These reactions create a modified polymer and the process has been termed photo-yellowing for low photon fluxes, e.g., sunlight, and incubation for ablation conditions. Incubation describes the chemical and physical changes in

Thomas Lippert was born in Germany where he studied chemistry at the University of Bayreuth. He received his Diploma in Ecological Chemistry (in 1990) and his Ph.D. in Physical Chemistry (in 1993) under Professor Alexander Wokaun. He did postdoctoral studies for Wacker Chemistry (Burghausen, Germany) and went then as a STA/Alexander von Humboldt postdoctoral fellow to Tsukuba, Japan (in 1994), where he worked at the National Institute of Materials and Chemical Research with Dr. Akira Yabe. He moved then as postdoctoral fellow (in 1995) to Los Alamos National Laboratory (Los Alamos, NM, USA) where he later became a Director's Postdoctoral Fellow and Technical Staff Member. He then joined the Paul Scherrer Institut (Villigen, Switzerland) as Senior Scientist (in 1999), and is currently the head of a research group. He received his Habilitation at the ETH Zuerich in Physical Chemistry (in 2002), where he is also a faculty member. His work has been focused on the design of novel polymers, ultrafast spectroscopy, thin film deposition, and microstructuring/surface modification. Lippert is author or co-author of over 120 technical articles including several book chapters. He has presented more than 50 invited talks on areas of laser interactions with materials and has organized several international conferences.

 © 2005 WILEY-VCH Verlag GmbH & Co. KGaA, Weinheim

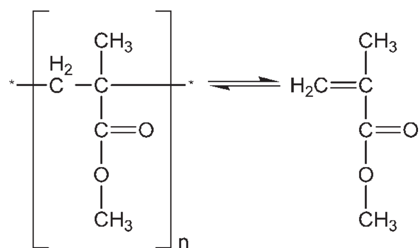

Figure 1. Chemical structure of PMMA and of its monomer.

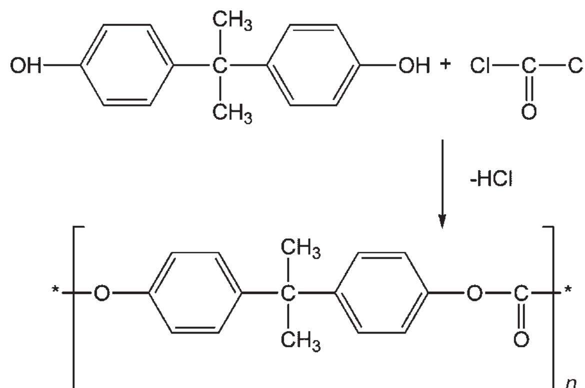

Figure 2. Chemical structure of a polycarbonate and of its monomers.

the polymer prior to ablation, i.e., mainly an increase of the absorption at the irradiation wavelength. The final step of the PMMA decomposition is the unzipping of the polymer (shown in step 4 of Figure 4), to yield the monomer.

It is worth mentioning that one chain end radical (as shown in Figure 4, step 3) will yield around 6 monomers at room temperature and over 200 at temperatures above the glass transition temperature T_g (378 K). This unzipping reaction is also observed for other polymers such as Teflon® and polystyrene. The small fragments in step 2, i.e., CH_4, CO, and CH_3OH, the detection of the monomer, and of the double bonds (chain end or in-chain) upon incubation and laser ablation are again clear indications for the involvement of photochemical reactions in the laser ablation process of PMMA. One other important fact is the difference of the products for UV and IR laser irradiation of PMMA. Upon irradiation with a CO_2 laser, the monomer is the exclusive product.[20] This is a clear indication of a purely thermal process, i.e., heating of the polymer above the ceiling temperature, whereas UV irradiation yields a rather broad mixture of products.

The pronounced differences in the ablation products between UV and mid-IR irradiation and clear indicators of a photochemical reaction in PMMA strongly suggest that the clear distinction of the ablation mechanism into photothermal and photochemical is at least questionable for UV laser ablation.

Photochemical decomposition of PMMA which alters the chemical structure will also result in a modification of the refractive index n.[21] This has been used to create planar waveguide structures within such polymers by applying low fluence irradiation at 248 nm.[22] The characteristics of the waveguide performance is at least quite promising.[22,23] Clear photothermal decomposition of PMMA upon CO_2

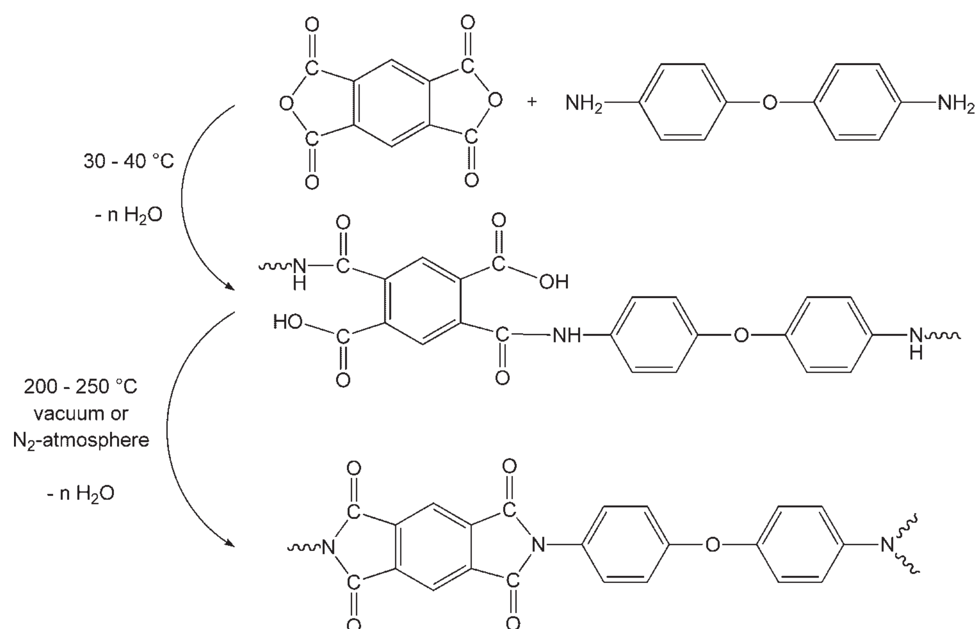

Figure 3. Chemical structure of a polyimide ((Kapton™), its intermediate (poly(amic acid)) and of the monomers (oxydianiline and pyromellitic dianhydride).

© 2005 WILEY-VCH Verlag GmbH & Co. KGaA, Weinheim

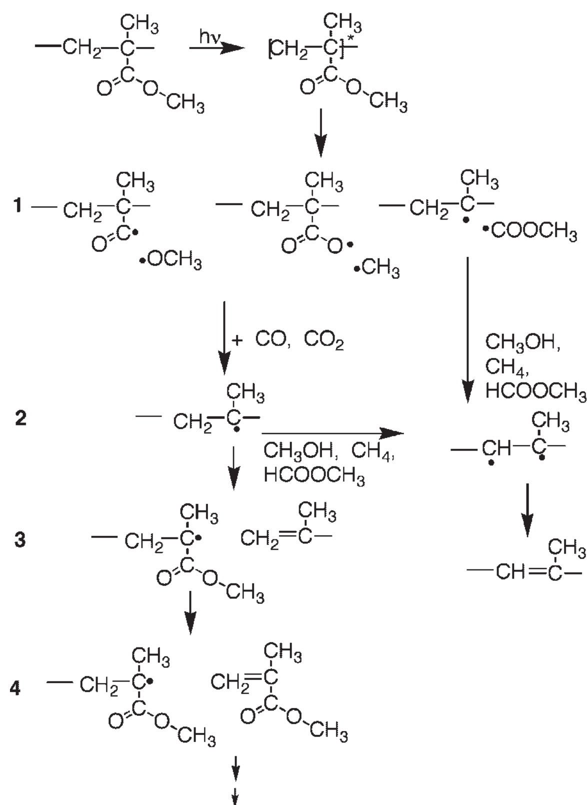

Figure 4. Photochemical decomposition pathway of PMMA.

laser irradiation has also been applied to economically fabricate microfluidic channels in PMMA.[24]

Laser Ablation of Polymers

In an attempt to study the ablation mechanism of PMMA and to apply longer irradiation wavelengths, i.e., 308 nm, which may be economically more interesting, various dopants have been tested to induce absorption at this wavelength. These dopants range from polycyclic aromatic compounds, such as pyrene, to compounds which contain a photochemically active group.[25] The utilization of dopants also allows decoupling of the absorption site, i.e., the dopant, from the polymer main chain. The polycyclic aromatic compounds reveal a photothermal mechanism which has been modeled by a cyclic multiphoton absorption mechanism where the triplet states play a key role.[26] The photochemically active compounds have been selected to test whether the dopant properties have a pronounced influence on the ablation mechanism. For these studies, various dopants based on the triazene group (–N=N–N<) have been tested. They are photochemically well studied[27–29] and release a large amount of nitrogen during the photochemical decomposition. It has also been suggested that the nitrogen, or other released gases, may act as a driving force in the ablation, carrying larger ablation fragments away from the surface. A detailed study of the ablation properties of PMMA doped with these triazene compounds revealed that very high ablation rates of up to 80 micro;m per pulse could be reached at high laser fluences and low doping levels, i.e., 0.5 to 1 wt.-%. A weak relation between the photochemical activity, i.e., the quantum yield, and the ablation rates was suggested.[30] A clear sign for the release of the gaseous products, i.e., mainly nitrogen, was detected in scanning electron micrographs (SEMs), which revealed a pronounced swelling (shown in Figure 5a). Structures with up to 200 μm of height are detected for fluences just below the ablation threshold. SEM images above the threshold of ablation show clear indications for the ejection of molten fragments, which are visible as fibers in Figure 5 (left). These fibers are of course an indication for a pronounced thermal part in the ablation mechanism, suggesting that these experiments using photochemical active dopants are not conclusive to prove a photochemical part in the ablation mechanism. Additionally, the quality of the ablation structures is not satisfactory due to the high roughness in the ablation craters, the ill-defined rims, and the large amount of ablation products surrounding the structures.

One reason for these features could be a low dopant concentration and correspondingly low absorption coefficients associated with the doped polymers. Doping of polymers with small molecules is unfortunately limited to ≈10 wt.-%. This is already accompanied by a significant

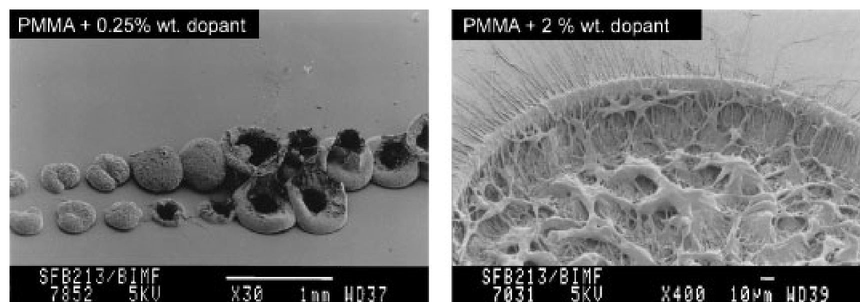

Figure 5. SEM photos of doped PMMA irradiated at 308 nm: left, 0.25 wt.-% of triazene dopant; right, 2 wt.-% of triazene dopant.

 © 2005 WILEY-VCH Verlag GmbH & Co. KGaA, Weinheim

decrease of the T_g of the polymers. Higher doping levels can also result in an agglomeration of the dopant, which may cause inhomogeneous ablation. Therefore, new polymers were developed which had the photolabile triazene group within the polymer main chain, with even two triazene chromophores in each repetition unit. This approach has several distinct advantages:

- the possibility to evaluate the influence of photochemical reactions on the ablation properties by tailoring the polymer;
- the chance to overcome some of the drawbacks of laser ablation that are normally observed for standard polymers. These drawbacks are the pronounced carbonization of the ablated surface and the redeposition of ablation products in the vicinity of and inside of the ablation craters.

The designed triazene-containing polymers, TP, (general structural unit shown in Figure 6 top) reveal several unique features. The absorption maximum and absorption coefficient can be tuned to certain wavelengths by varying "X" in Figure 6.[31] This allows their absorption coefficients to be matched with those of other polymers that are used for comparison, e.g., polyimide, Kapton™ (structure shown in Figure 6 bottom). The absorption maximum of the TP can be tuned from 290 to 360 nm with maximum linear absorption coefficients, α_{lin}, reaching almost 200 000 cm^{-1}. Typical absorption spectra of a triazene and a polyimide polymer are shown in Figure 7.

The spectrum also reveals one of the most interesting properties of triazene polymers, i.e., the two absorption maxima that can be clearly assigned to the aromatic system (around 200 nm) and the triazene unit (around 330 nm).[32] This allows selective excitation of various polymer chromophores by switching from 193 to 248 or 308 nm irradiation.

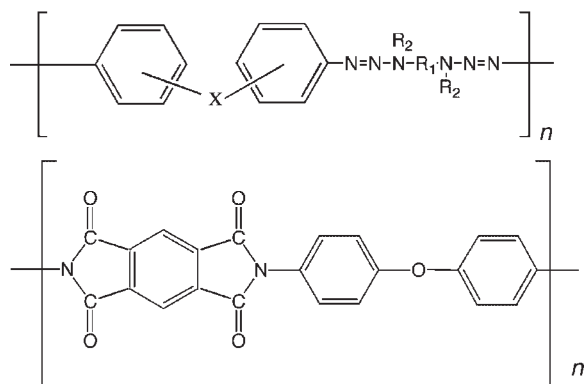

Figure 6. Chemical structures of the triazene polymers and of polyimide (Kapton™).

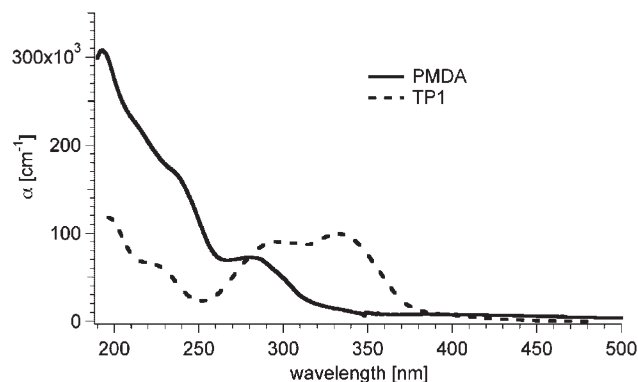

Figure 7. UV-Vis absorption spectra of thin films of a triazene polymer (structure shown in Figure 8) and of a polyimide (PMDA, structure shown in Figure 12).

Ablation of Polyimides and Triazene Polymers

A detailed comparison of the ablation rates of a polyimide, PI (i.e., Kapton HN), and the triazene polymer (with the chemical structure shown in Figure 8) is shown in Figure 9 for irradiation at 308 nm. Here both polymers exhibit almost the same linear absorption coefficients. This data was analyzed from multi-pulse experiments on one given sample by measuring the ablation depth for each given fluence and pulse number. The slope of the ablation depth versus pulse number plot corresponds to the ablation rate at a given fluence. The effective absorption coefficient α_{eff} was calculated according to Equation (1) (see below). Both polymers reveal a quite complex ablation behavior characterized by the changing α_{eff}. These changes may be described by several linear relations which indicate changes in the ablation process or mechanisms. The linear ranges can be used to calculate α_{eff} which suggest in the case of TP and also for PI (Kapton™), that over the whole fluence range a pronounced bleaching is observed (lower α_{eff} than α_{lin}).[31,33,34]

This results in larger laser penetration depths and therefore higher ablation rates than predicted by the absorption coefficients. Such a bleaching process is more pronounced for TP in the low fluence range than for PI, but increases for both polymers with increasing fluences. At the highest fluences this trend seems to change in the case of TP, where a slight increase of α_{eff} is observed, which is assigned to plasma absorption (plasma shielding).[34] The differences between the two polymers in the low fluence range are most

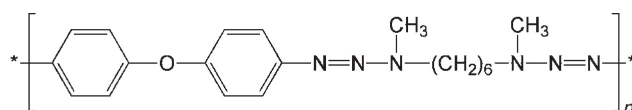

Figure 8. Chemical structure of the triazene polymer TP1 which was used for the UV-Vis absorption spectra and most ablation experiments.

© 2005 WILEY-VCH Verlag GmbH & Co. KGaA, Weinheim

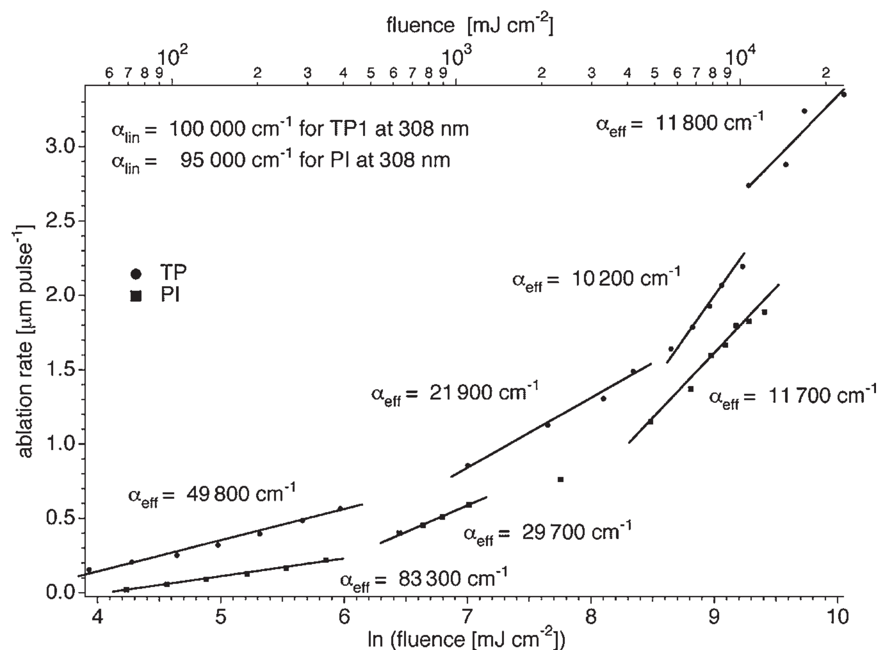

Figure 9. Ablation rates versus laser fluence for TP1 and Kapton^{TM}, including the linear fits according to Equation (1) to obtain the effective absorption coefficients, α_{eff}.

probably due to the more efficient photochemical decomposition of the TP during the laser pulse. Another interesting difference between these polymers is the quality of the ablated structures. The TP can be structured at this irradiation wavelength of 308 nm with high quality and without any visible redeposited ablation products or modification of the ablated polymer surface. Test pattern ablated into TP (left) and Kapton^{TM} are compared in Figure 10. The structure in TP is much sharper and the re-deposited carbon material that is clearly visible in the case of PI is absent. This modification of the surface has been studied for both materials using various analytical tools, such as X-ray photoelectron spectroscopy (XPS) and confocal Raman microscopy. Surface analysis after irradiation at fluences above and below the ablation threshold of 20 $mJ \cdot cm^{-2}$ (i.e., at 10 $mJ \cdot cm^{-2}$ and 30 $mJ \cdot cm^{-2}$) reveal pronounced differences for the irradiation of TP.[35,36] Surface modification at fluences below the ablation threshold is solely chemical for irradiation at 308 nm (also for 248 nm) and can be assigned to an oxidation of the surface. The oxidation is confirmed by a decrease of the nitrogen signals and an increase in the oxygen signals in XPS measurements. Oxidation also decreases the contact angle of water droplets in the irradiated area. SEM inspection revealed no physical change of the surface at fluences below the ablation threshold. Surface modification at fluences above the ablation threshold clearly depends on the irradiation wavelength. At 308 nm, the chemical composition of the polymer surface remains unchanged after several pulses, consistent with a photochemical mechanism where the polymer is removed completely layer by layer without re-deposition of ablation products. In the case of 248 nm irradiation a pronounced carbonization of the surface is detected. This suggests that excitation of the triazene chromophore with irradiation at

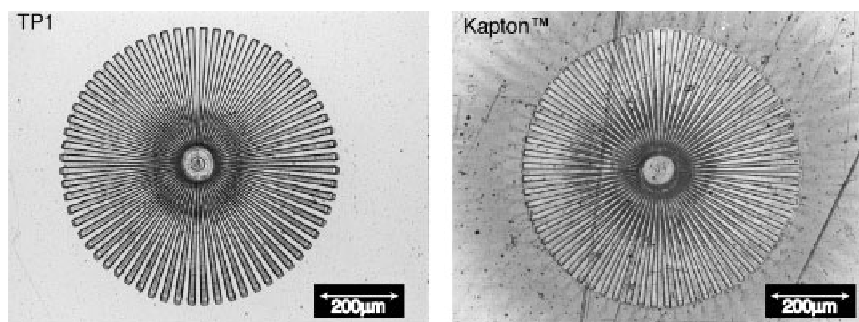

Figure 10. Ablation pattern in TP1 (left) and Kapton^{TM} (right) created by 308 nm irradiation using a gray tone phase mask.

 © 2005 WILEY-VCH Verlag GmbH & Co. KGaA, Weinheim

308 nm results in the decomposition of the triazene group and a pronounced removal of intact aromatic groups. Irradiation at 248 nm excites the triazene group and the aromatic system (see UV-Vis spectrum in Figure 7) and results in the decomposition of the triazene group and of aromatic groups that yield the C_x^y species which are responsible for carbonization. Modification of the surface composition of Kapton™ has been analyzed in detail by XPS[37] and confocal Raman microscopy.[38] The data clearly show that the ablation structures are surrounded by a carbon layer whose thickness depends on the applied fluence and number of pulses. Carbonization was also detected inside the structures, but with a slightly higher degree of crystallinity for the carbon.[37]

In this context it is worth mentioning that "polyimide" (PI) is probably the most studied polymer in laser ablation. PI is also the material for which most ablation models are applied, but great care has to be taken for which type of PI the data have been obtained. PI is not a single polymer, but describes a class of polymers which contain at least one cyclic imide group (shown in Figure 11) per repetition unit. Even Kapton™ is not one polymer, but there are also many different types of Kapton™ which are defined with additional letters, e.g., HN.

Most studies are probably performed for one type of Kapton™, i.e., HN, which is fabricated by DuPont in the form of sheets. Another very similar type of polyimide is Upilex™ from Ube Industries which has also been used in ablation studies.[39,40] Both of these polymers are available as sheets in a wide variety of thickness, but they are both insoluble. Soluble types of PI have been applied in all experiments where it is necessary to produce thin films on substrates.[41,42] The polymers can be processed as thin films because they are delivered in solution as poly(amic acid) (see Figure 3) and imidization to form films takes place on the substrate. One of these types of PI, i.e., PMDA (chemical structure shown in Figure 12), was used for the UV-Vis spectrum in Figure 7. These polyimides probably still have properties that are quite similar to Kapton™ while another class of soluble PIs is classified as photosensitive PIs, e.g., Pyralin™ or Durimid™ (chemical structure shown in Figure 10). These materials behave very differently compared to non-photosensitive PI, and reveal very different ablation rates and threshold fluences. It is worth noting that in a quartz micro balance (QMB) study of PI

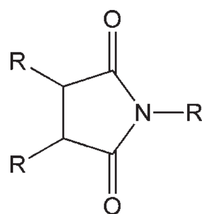

Figure 11. Chemical structure of a succinimide unit.

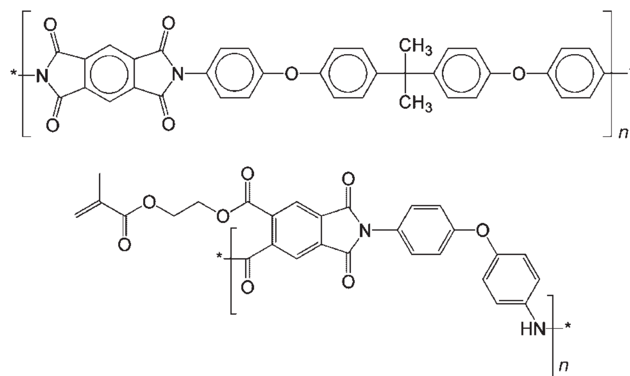

Figure 12. Chemical structures of PMDA (top) and Durimid™ (bottom).

ablation rates Pyralin™ was used as sample.[43] This ablation data has been used for modeling ablation rates, but applying the material properties of Kapton™[9] which are well-known, contrary to the properties for many other types of PI.

When comparing ablation data it is also important to be very careful, as the usual ablation parameter, such as ablation rate, d(f), threshold fluence, F_{th}, and effective absorption coefficient, α_{eff}, are strongly influenced by the method that is applied for determining these values. The usual way to obtain these values is by applying the following empirical Equation (1)[44,45] to the ablation rates:

$$d(\mathrm{F}) = \frac{1}{\alpha_{eff}} \ln\left(\frac{F}{F_{th}}\right) \tag{1}$$

The ablation rate per pulse d(F) is plotted as a function of the logarithm of the laser fluence F and from the linear fits the threshold fluence F_{th}, and the effective absorption coefficient α_{eff} are obtained. The first fundamental issue is the ablation rate per pulse, and whether this is defined as an ablation rate for a single pulse, or as the slope of a plot where the ablation depth is plotted as function of the pulse numbers for a given fluence. These two different analytical methods can result in very different ablation rates, especially in the case of polymers which reveal incubation. Incubation is defined as the processes that are often accompanied by an increase of absorption, e.g., due to the double bonds in PMMA (see Figure 4) and which take place during irradiation or prior to the onset of ablation. This means for ablation that a certain number of pulses do not induce ablation, but instead lead only to chemical or physical modification. If the ablation rates include these incubation pulses, then of course different ablation rates are obtained compared to an analysis where only the pulses are used for which ablation is detected. Another problem in analyzing the ablation depth from multipulse experiments is the above described surface modification of the polymer which may alter the ablation rates with consecutive pulses. These difficulties can be overcome by utilizing only single pulse

© 2005 WILEY-VCH Verlag GmbH & Co. KGaA, Weinheim

ablation rates, which are of course more difficult to measure, as very sensitive techniques are needed. Unfortunately one problem may be encountered even for single pulse experiments which originates from an experimental procedure where consecutive pulses are delivered to the same position of the polymer. In the case of PI[46,47] and several other polymers chemical modifications are detected, which very often corresponds to carbonization of the polymer. The polymer with this carbonized layer exhibits a different ablation rate, due to the different material properties of this composite material, which are not comparable to the original polymer.

It is also necessary to consider that physical changes of the polymer surface, i.e., an increase of roughness, can cause problems. An increase of roughness corresponds to an increase of the surface area, which results in an decrease of laser fluence that can even terminate ablation when the fluence decreases below the ablation threshold.[48] The last point that has to be considered is the method of measuring the ablation depth. This can be done by ''mechanical'' methods with a tip, e.g., profilometry or atomic force microscopy (AFM), where changes of the surface morphology are detected. Another method is a gravimetric method, i.e., quartz crystal microbalance (QMB), where the weight loss is measured. The latter can and will also detect reactions inside the polymer layer which are associated with a weight loss, e.g., loss of N_2 for the triazene polymer. The reaction may not be accompanied by the creation of an ablation crater that is measured by the ''mechanical'' methods. The influence of chemical and/or physical changes of the polymer surface arising from multi-pulse irradiation is clearly visible in Figure 13 and 14, where the ablation rates, determined by QMB, of PMDA for 193 nm irradiation and TP for 248 nm irradiation are shown as a function of the pulse numbers. The ablation rates decrease with the number of pulses delivered to the sample surface prior to the measurements.[49] A pronounced carbonization was detected for both polymers at these irradiation wavelengths. To obtain ''true'' ablation rates it is therefore not only necessary to apply single pulses but also to utilize a new sample for each experiment, which again may be problematic, as in the case of PMMA a skin layer with different ablation properties is formed for solvent cast films.[19] The data in Figure 15 and 16 correspond to true single pulse experiments where the ablation rate was determined by QMB and where for each measurements point a new sample was used. The difference between the ablation rates of a photosensitive polyimide, i.e., Durimid™, and a standard polyimide, i.e., PMDA, are shown for two different irradiation wavelengths in Figure 15 (193 nm) and 16 (308 nm). For the irradiation wavelength of 193 nm (Figure 15) at least similar ablation rates of the single pulse experiments were obtained, while for an irradiation wavelength of 308 nm extremely different data are derived. This is of course problematical if data from QMB experiments and photosensitive polyimides, such as Durimid™ (which behaves probably very similar to Pyralin™), are used for modeling the ablation of Kapton™. The photosensitive PIs reveal very different ablation rates and probably also have

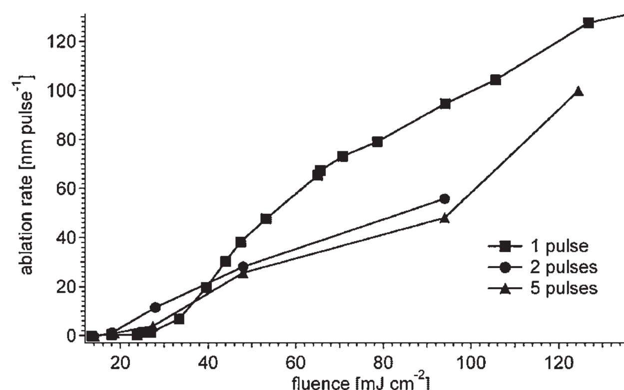

Figure 14. Ablation rates of TP1 for 248 nm irradiation with variable pulse numbers measured by QMB.

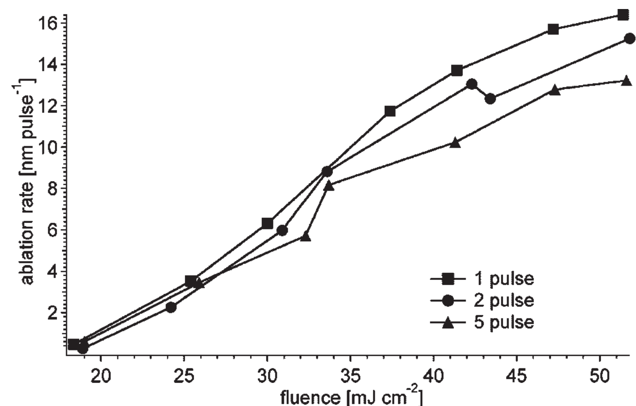

Figure 13. Ablation rates of PMDA for 193 nm irradiation with variable pulse numbers measured by QMB.

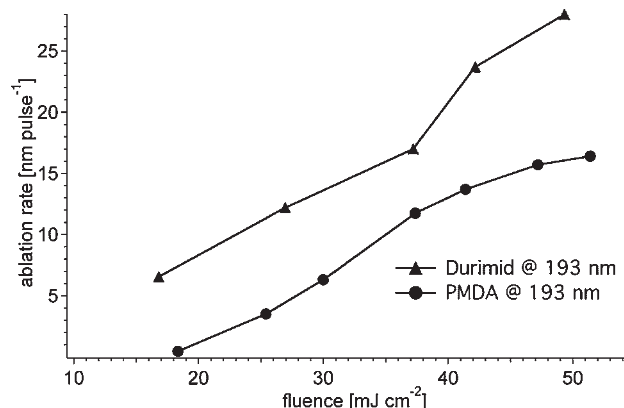

Figure 15. Ablation rates of PMDA and Durimid™ for 193 nm irradiation with single pulses measured by QMB.

© 2005 WILEY-VCH Verlag GmbH & Co. KGaA, Weinheim

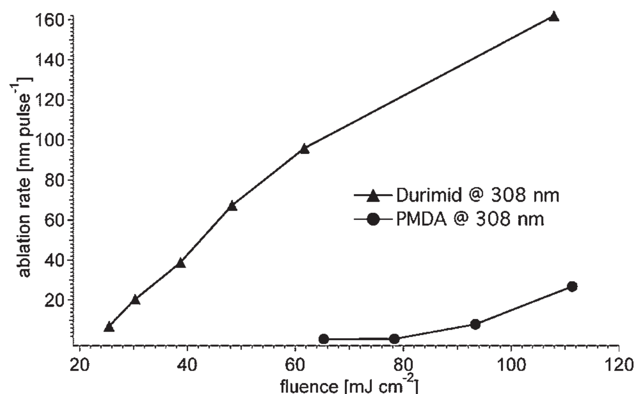

Figure 16. Ablation rates of PMDA and Durimid™ for 308 nm irradiation with single pulses measured by QMB.

different material constants. It is worth mentioning that in the case of the irradiation of TP1 at 308 nm profilometric measurements yield the same ablation rates as those obtained from the QMB data.

The single pulse data of Durimid™ did also not reveal the pronounced so-called Arrhenius tail in the ablation data for irradiation at 308 nm (see Figure 16), which has been observed previously for the similar Pyralin™[43] and which has been interpreted in detail by some models.[9] This Arrhenius tail is normally described by a smooth exponential increase of the ablation rates with laser fluence. These rates corresponding to the low ablation rates at low fluences were modeled using an Arrhenius-type rate equation. The absence of the Arrhenius tail for 308 nm irradiation may be due to the above mentioned chemical modification upon consecutive irradiation of the same polymer sample. These modifications affect the Pyralin™ data obtained via QMB measurements using with several pulses at each sample position (starting even with the high fluences). The pronounced difference between the ablation rates of the photosensitive polyimide and standard polyimides, such as PMDA, also implies that it is very important to consider which type of polyimide is used in the measurements and of course how the ablation data, e.g., ablation rates, were obtained.

Ablation Mechanisms

Various approaches to obtain a better understanding of the ablation mechanisms have been developed and may be divided into three different methods:

- Changing the polymer structure
- Time-resolved measurements during ablation and
- Varying the laser pulse lengths and wavelengths.

In an approach to improve the chemical stability of triazene polymers and to probe the influence of the chemical structure on ablation, alternative polymers have been developed. These polymers still contain the photochemical active groups that release gaseous products upon irradiation. These structures are based on a malonyl-ester group (MP, shown in Figure 17) which also contains a double bond that can be utilized for a cross-linking reaction (Figure 17). This also allows analysis of the influence of cross-linking on the ablation properties. Cross-linked polymers are labeled with the additional letter "C" following the polymer acronyms (e.g., in Figure 19). Ablation rates associated with these polymers are well below the values obtained for the triazene polymers. Therefore polymers were developed that contained both groups, i.e., the triazene group and the malonyl-ester group, in the repetition unit of the polymer (TM-polymers, shown in Figure 18). These polymers allow an investigation of the influence of cross-linking and the influence of the linear absorption coefficient by varying R in the chemical structures (Figure 17 and 18).[50–53]

A summary of the ablation behavior is given in Figure 19, where the ablation rates at a fluence of 100 $mJ \cdot cm^{-2}$ for irradiation at 308 nm are shown for various polymers. Here MP 1 and 2 are two different malonyl-ester polymers with different absorption coefficients, TP is the triazene polymer from Figure 6, PI is Kapton™ (Figure 6), PEST is a commercial polyester, and TM are the combined malonyl-ester-triazene polymers. The ablation rates clearly show that the polymers can be roughly divided into two groups. All polymers containing the photochemical most sensitive triazene group reveal much higher ablation rates (up to 250 nm per pulse) than other polymers which show ablation rates in the range of 60 to 130 nm.

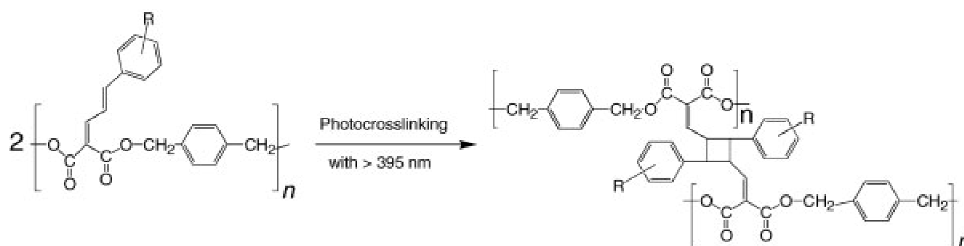

Figure 17. Chemical structure of the malonyl-ester polymer (MP) with a side chain double bond which is used for cross linking.

© 2005 WILEY-VCH Verlag GmbH & Co. KGaA, Weinheim

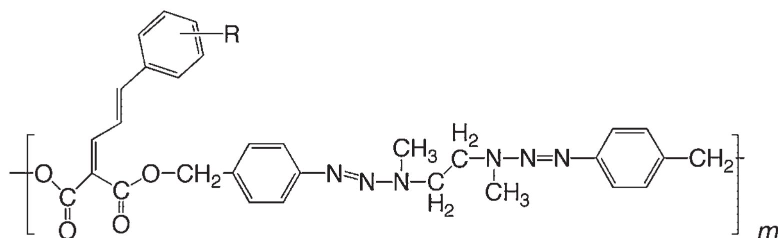

Figure 18. Chemical structure of the polymer TM that combines the triazene and malonyl ester functionality.

The also photochemically active MP polymers exhibit still higher ablation rates than the two standard polymers, i.e., PI and PEST. Cross-linking of the polymers, and therefore changing of certain polymer properties such as solubility, mechanical properties, and T_g, seem to have only minor influence on the ablation rates. However, these cross-linked polymers consistently exhibit ablation rates which are slightly lower than the standard polymers. It appears that the most important influence on the ablation rate and on the threshold fluence, but with an inverse behavior, i.e., lower thresholds for the triazene group containing polymers, is the chemical structure of the polymers. The absorption coefficients are within the tested range only of minor importance. It is worth mentioning that TP, the triazene polymer with the highest density of the photochemical active triazene groups per repetition unit, reveals the highest ablation rate. The order of the ablation rates follows quite well the order of photochemical decomposition in solution using low fluences and low concentrations of the polymer (in the range of 10^{-5} mol · l^{-1}).[50] Excimer lamps were alternatively employed to study the effect of low fluence irradiation at 222 and 308 nm, where linear (no ablation) photochemistry is expected.[54] Excimer lamps emit incoherent, quasi-continuous radiation at the same wavelength as the excimer laser. At low photon fluxes provided by the lamps, multi-photon processes can be neglected. Decomposition of the triazene chromophore was detected by UV-spectroscopy for 222 and 308 nm irradiation, while decomposition of the aromatic chromophore was detected only at 222 nm. This is consistent with the absence of surface carbonization for irradiation at 308 nm and the detection of carbonization for irradiation at 248 nm. The triazene-chromophore decomposes at fluences well below the ablation threshold and is clearly the most sensitive chromophore in the triazene-polymer that decomposes directly during irradiation at 308 nm. The ablation data suggest also that photochemical activity and therefore the possibility of a photochemical part in the ablation mechanism is at least likely.

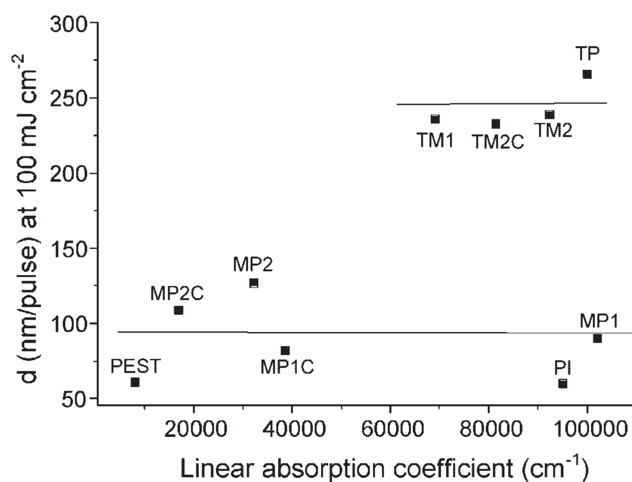

Figure 19. Comparison of the ablation rates for 308 nm irradiation of various polymers using a fluence of 100 mJ · cm^{-2}.

Therefore one triazene polymer, i.e., TP1 (Figure 8) was selected for analysis by various time-resolved techniques during and directly after irradiation at 308 nm and 248 nm. The following techniques have been applied to probe the ablation mechanism:

- Time resolved transmission
- ns shadowgraphy
- ns surface interferometry and
- Time-of-flight mass spectrometry (ToF-MS).

In an attempt to account for the different ablation behavior at 308 and 248 nm, i.e., the different surface modification[35,36] and the lower ablation rates for 248 nm irradiation,[33] time resolved transmission experiments were performed. An increase in transmission with increasing fluences was observed for 248 and 308 nm irradiation, suggesting the presence of a bleaching process at higher fluences.[32,55] In principle, this bleaching could be transient or permanent (i.e., decomposition). A higher degree of transmission increase was detected for irradiation at 308 nm which can account for the higher ablation rates at this wavelength.

To address the issue of a possible photothermal contribution to the ablation mechanism, a nanosecond (ns) imaging technique[56–59] was employed that produces a series of shadowgraphs of the air-polymer interface. Two different experimental techniques were employed, which have been described in detail elsewhere.[60] Briefly, direct imaging of the shockwave and ablation products has been utilized which yields very clear images (Figure 20 right), and an

© 2005 WILEY-VCH Verlag GmbH & Co. KGaA, Weinheim

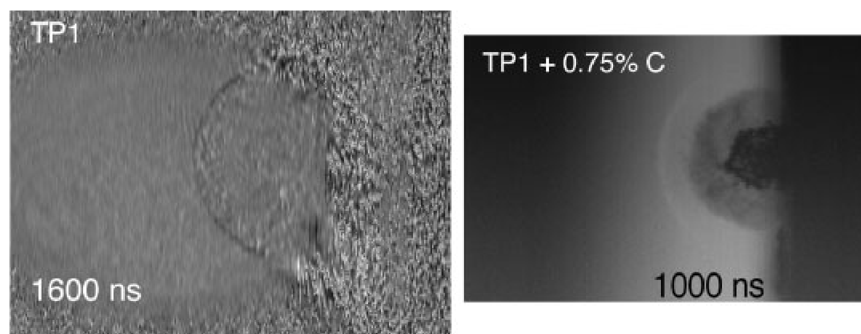

Figure 20. Shock waves created by irradiation of TP1 in air. Left picture obtained by a Mach-Zehnder interferometric setup: 308 nm irradiation; right picture obtained by direct imaging: 1 064 nm irradiation of a carbon doped TP1.

interferometric setup which allows a better analysis of the shockwave although the images look less clear (Figure 20 left). The pictures clearly show the shockwave in air and confirm the absence of solid products for irradiation at 308 nm (Figure 20 left), which has been expected from the absence of re-deposited material. For comparison, a shadowgraphy picture using carbon as dopant and 1 064 nm irradiation is included (Figure 20 right), which shows a large amount of solid ablation products. The advance of the supersonic shock waves can be modeled by a model of the blast wave which incorporates the mass of the ablated polymer and the decomposition enthalpy of the polymer.[61] Irradiation at 193 nm yields faster shockwave velocities than irradiation at 308 nm, despite the similar absorption coefficient, presumably due to the more efficient polymer fragmentation by the high-energy, 193-nm photons. The larger number of small molecules at 193 nm results in higher pressures and therefore faster shockwaves.[62] A comparison of the shock wave expansion is shown in Figure 21. The shock wave velocity for 1 064 nm irradiation of the carbon doped TP1 is also included. It was necessary to increase the laser fluence at this wavelength by 10 times

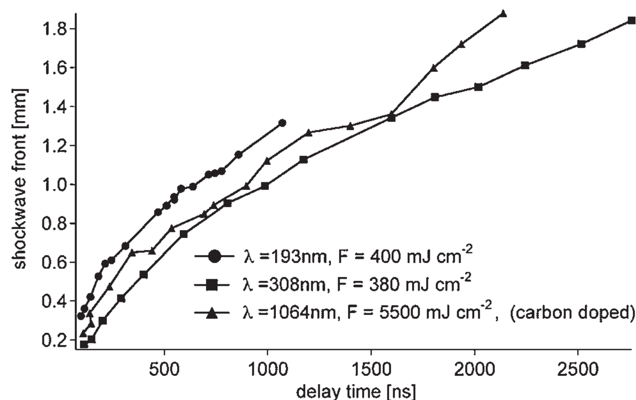

Figure 21. Comparison of the shock wave expansions for TP1 at different irradiation wavelengths.

to obtain similar expansion velocities as for the UV irradiation wavelengths. This is most probably due to the fact that the carbon doped TP has a much higher threshold fluence for irradiation at 1 064 nm and that the amount of gaseous products is much lower and large amounts of solid products are ejected (shown in Figure 20).

Shadowgraph imaging was supplemented by ns-surface interferometry.[58,63,64] Interferometric images (shown in Figure 22) can reveal changes in surface morphology on ns-timescales, both during and after the laser pulse. Some of these changes are potentially related to photochemical and photothermal ablation mechanisms: photothermal ablation is often associated with a pronounced surface swelling and delayed material ejection, while photochemical ablation in many cases yields instantaneous etching. This is especially the case for excited states with short life times (10^{-12}–10^{-10} s). Examples of two interferometric images are shown in Figure 22 (top). The left image is recorded prior to irradiation and is used as reference, while the image on the right corresponds to the time resolved image which is used for the analysis. The analysis of the images is performed by applying a fast Fourier transform (FFT) routine that includes digital filtering. The results of the analysis are phase shift information that correspond to ablation or swelling while the amplitude information is equal to changes of the reflectivity. Interferometric images of TP at 193, 308[62,65] and 351 nm[64] show that etching of the film begins and ends with the laser pulse (shown in Figure 22 for 308 nm irradiation). In contrast, corresponding images of polyimide for irradiation at 351 nm reveal pronounced swelling, followed by material removal that persists for several μs after the laser pulse.[41,42]

Significantly, surface reflectivity measurements (probed at 532 nm) during ablation at 308 nm show a decrease in reflectivity (darkening) during the laser pulse (included in Figure 22) which recovers completely after the laser pulse.[64]

Insight into the ablation mechanisms is also provided by studying the ablation products, e.g., by MS. It is worth

 © 2005 WILEY-VCH Verlag GmbH & Co. KGaA, Weinheim

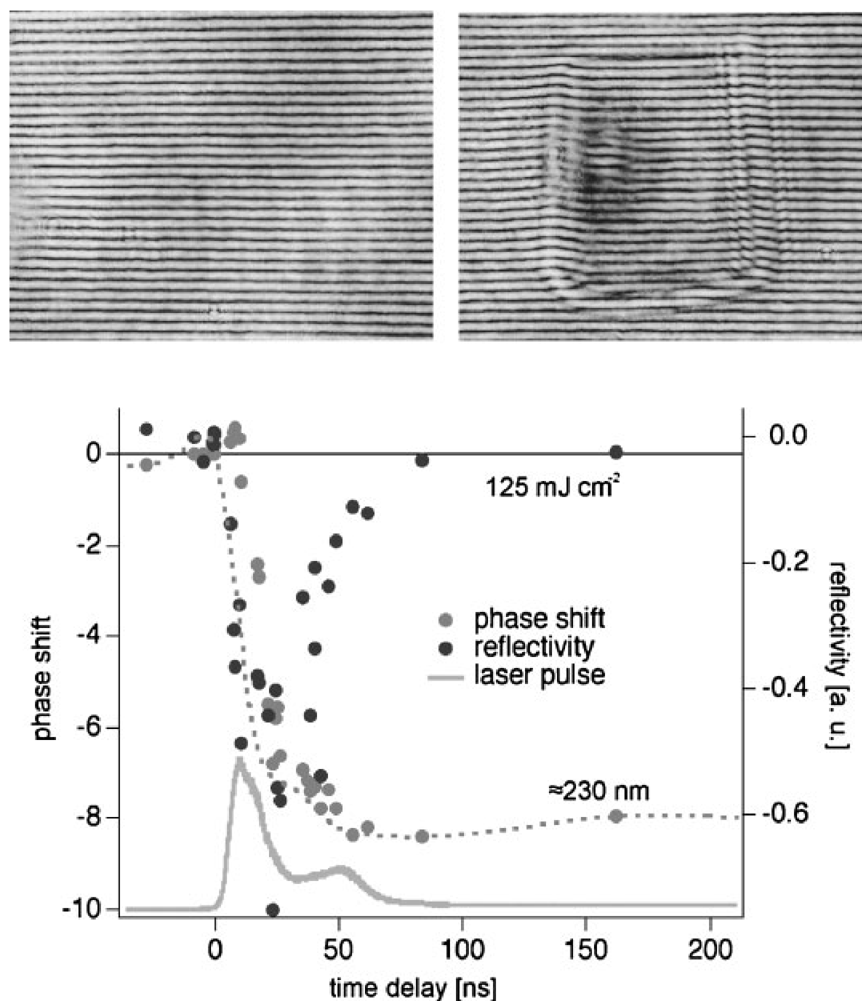

Figure 22. Surface interferometric analysis of the ablation process for TP1 and an irradiation wavelength of 308 nm. Top left: interference image prior to irradiation; top right: interference image after a delay time of 160 ns. Bottom: analysis of a complete set of interferometric images using a FFT routine which yields the phase shift (depth) and reflectivity.

mentioning that time-resolved MS at 248 and 308 nm irradiation identified all the expected fragments of the decomposition of TP1 (shown in Figure 23),[54,66,67] but it should also be noted that thermal decomposition yields similar products.[68] Importantly, three different species of nitrogen were detected in the ToF-signals (shown in Figure 24), including a very fast ground state neutral (up to 6 eV of kinetic energy), a slower neutral ground state species with a broad energy distribution (probably a thermal product), and possibly a metastable (excited) neutral N_2 species.[69] The latter can only be created by an electronic excitation. The ToF curves for a commercial polymer, i.e., Teflon®, after irradiation at 248 nm reveals unzipping, where the main product of decomposition is the monomer (mass 100, C_2F_4). The ToF curve in Figure 24 includes the modeling of the data using a Maxwell-Boltzmann distribution which yields a temperature of 987 K that is at least compatible with the decomposition (>673 K) and ceiling temperature (≈1 200 K) of Teflon®.[70]

The data for the photochemically active polymer (TP1) strongly suggest that photochemistry can play an important role in the ablation mechanism of polymers, but it is also clear that photothermally induced reactions are important. This is for example confirmed by the presence of a thermal N_2 product in the ToF curves. A photothermal mechanism will always be present, especially when the polymers decompose exothermically during photochemical decomposition and if the quantum yields of the photochemical reactions are not equal to 1. Ablation of polymers will therefore always be a mixture of photochemical and photothermal reactions, where the ratio between these two is influenced by the material, i.e., mainly thermal for polymers such as Teflon® and with more pronounced photochemical features for photoactive polymers. The photochemical

 © 2005 WILEY-VCH Verlag GmbH & Co. KGaA, Weinheim

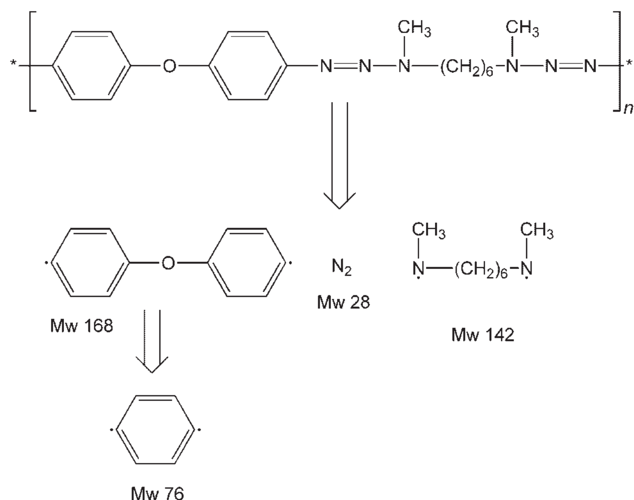

Figure 23. Decomposition pathway for TP1 after 308 nm irradiation with all fragments that were observed in ToF-MS measurements.

features are, e.g., the bleaching of the triazene chromophore during the pulse, the ablation starting and ending with the laser pulse, and the very fast or metastable ablation products.

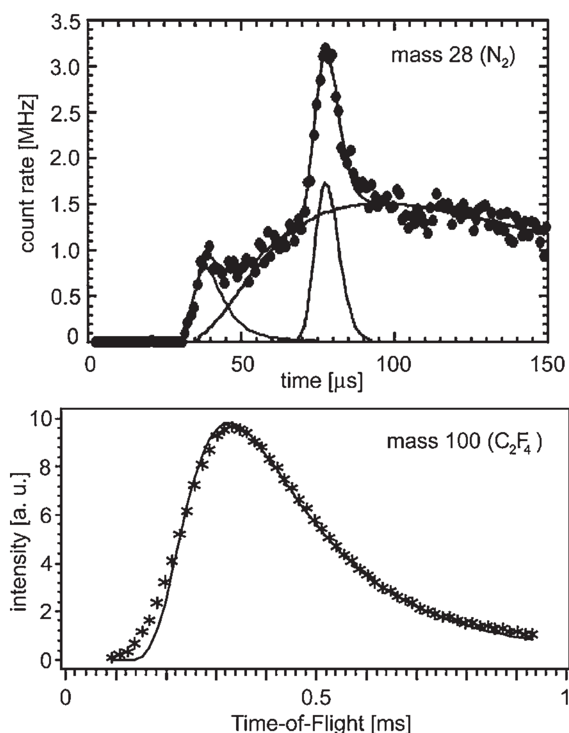

Figure 24. ToF curve for mass 28 obtained for 308 nm irradiation of TP1 (top) and mass 100 obtained for 248 nm irradiation of Teflon®.

Other Approaches for Analyzing the Mechanism of Ablation

Variation of Pulse Length

Bäuerle et al.[6] have emphasized the value of single-pulse ablation studies as a function of pulse length, with tightly focused beams, for revealing the ablation mechanisms. Under these conditions the photochemical processes should depend on the product of intensity (I) and pulse length (τ_1), while photothermal and photophysical processes should depend more strongly on τ_1. Single pulse laser experiments for a polyimide at 302 nm (Ar ion laser irradiation) and pulse lengths between 140 ns and 50 ms have been performed.[71–73] The changes in surface topology and the crater depths were analysed by AFM. With an increase of the pulse length, the threshold fluence increases in a power law fashion, which is consistent with a thermal model.[74] These data strongly support a thermal decomposition mechanism for PI, at least for pulses longer than 100 ns, which is much longer than the typical pulse length of excimer lasers (10–30 ns).

Ablation Studies Using Various Irradiation Sources

Continuous-Wave UV Lasers

Continuous wave (CW) UV lasers were also applied to structure various commercial polymers, such as PMMA, poly(ethylene terephthalate) (PET), and PI, either by scanning the beam across the surface with transit times over the beam diameter of 1–1 000 µs or by mechanically chopping the beam to obtain 10–400 µs pulses. In the case of PI, the fluences required for etching are similar to the fluences employed with excimer lasers, but typical etch depths per joule are about 100-fold less.[75] Etching is observed only when the laser beam is translated across the sample. Irradiation at a single position merely blackens and swells the surface. By chopping the laser beam (350 µs pulses) holes can be drilled in PI. Although the walls of the hole are heavily carbonized, no signs of debris are observed.[76] A chemical transformation which yields carbon in a form similar to glassy carbon is observed for irradiation with very long (millisecond) pulses.[77]

Structuring with these long pulses, or better, by scanning the CW-laser beam, apparently involves different processes than structuring with excimer lasers.

Ultrafast Lasers

With the development of chirped pulse amplification (CPA), IR solid state (Ti:sapphire) lasers have become compact, extremely high-brightness sources.[78] Material processing with femtosecond (fs) lasers is already an established technique. Ablation with fs pulses has unique advantages, including a negligible heat-affected zone, lower ablation threshold, absence of plasma shielding, and the ability to

 © 2005 WILEY-VCH Verlag GmbH & Co. KGaA, Weinheim

structure ''transparent'' materials. The rapid transfer of laser technology from experimental systems to industrial environments (as in mask repair[79,80]) has been astonishing. We have come a long way since the first reports of fs laser ablation of polymers in 1987 by Srinivasan et al.[81] and Stuke et al.[82]

Femtosecond Lasers

Only a brief description of fs laser ablation will be given here, as polymer ablation using fs laser has been recently reviewed.[83]

Srinivasan showed[81] that it is possible to produce high quality structures in PMMA with 160 fs pulses at 308 nm, whereas ns pulses at the same wavelength only ''damage'' the surface. Irradiation of PMMA with 300 fs, 248-nm laser pulses showed[82] that fs pulses have a threshold for structuring that is a factor of 5 lower compared to ns pulses, and that much better structures are produced. Femtosecond pulses also produce high quality structures in Teflon®,[84] with no signs of the thermal degradation associated with ns pulses.[85] Experimental data suggest that multi-photon absorption dominates the ablation process in PMMA and Teflon®.

Chirped-pulse Ti:sapphire systems were first applied to polymers in 1994[86] for the ablation of Teflon®, PI and perfluorinated poly(ethylene-*co*-propylene) (FEP). An interesting aspect of fs laser ablation has been obtained for the ablation of PI, PC, PET and PMMA[87–90] using 150-fs pulses at 800 nm. The single pulse threshold increases from 1 $J \cdot cm^{-2}$ for PI to 2.6 $J \cdot cm^{-2}$ for PMMA. The ablation thresholds correlate with the optical band gaps of these materials, consistent with multiphoton absorption. All polymers show pronounced incubation effects, with stronger incubation in PC, PET and PMMA relative to the more ''stable'' polymers PI (Kapton™) and Teflon®. The ablation crater of all polymers, except PI, show clear signs of melting and redeposition of molten material, in contrast with the clean ablation contours obtained by UV-fs laser ablation.[81] The absence of splashing for PI is not really surprising, as typically PI decomposes rather than melts. Interestingly, the etch rates for PI depend on the laser polarization.[87] Circular polarization yields slightly higher ablation rates than linear polarization.

Reversible microstructuring *inside* (10 µm below the surface) of *cis*-1,4-polybutadiene (PB) films has been observed with fs pulses.[91] The structures produced inside the film by single laser pulses were probed by optical transmission. Two different threshold fluences are observed: the ''normal'' threshold at the onset of ablation, and a second threshold, marking the onset of permanent structuring. Between these two thresholds, transmission changes recover on time scales of 10–100 s. Fluences above the second threshold permanently change the optical transmission. Doping PB with a photolabile compound (pentazadiene) lowers the (first) ablation threshold by 20%.

Time-resolved reflectivity measurements on PMMA and PS show reflectivity increases by factors of 1–5 after exposure to 500 fs laser pulses,[92,93] while the changes of reflectivity for a triazene polymer after irradiation are rather complex. Depending on the fluence, transient increases and decreases are observed on timescales from ns to µs.[94,95]

Picosecond Lasers

Picosecond (ps) pulses have not found many applications in structuring of polymers, as they lack the advantages of fs pulses, and perform not much better than ns pulses, at least in the UV. The effect of ps and ns pulses on PMMA has been studied in the UV (266 nm) and the near IR (1 064 nm)[96] using different dopants, i.e., IR-165 at 1 064 nm and diazomeldrum's acid (DMA) at 266 nm. With IR-165, the polymer matrix is heated by vibrational relaxation and multi-phonon up-pumping.[97] In the IR, 100-ps pulses produced clean etch features, while 6-ns pulses yielded rough surface features. This is consistent with the fast vibrational relaxation in IR-165, which allows for higher temperature jumps with ps pulses. In the UV, heating of DMA-doped PMMA is attributed to cyclic multi-photon absorption[98] and ablation was obtained only with the ns pulses, and even then only low quality features were obtained. Picosecond pulses merely swell the surface.

Dlott et al.[99–104] have performed several studies of ps ablation, with an emphasis on spectroscopy (coherent anti-Stokes Raman scattering (CARS), absorption, and ultrafast imaging) to elucidate the ablation mechanisms. It has been shown that ps pulses produce fast temperature jumps and solid-state shock waves, which are not produced by longer pulses. The pressure jumps, often several kbar, are produced when the film is heated faster than the characteristic hydrodynamic volume relaxation time. Pressure release occurs by the propagation of a rarefaction wave. The tensile forces generated when this rarefaction wave reaches the substrate can easily fracture the substrate-thin film bond. The pressure in the thin film at ablation threshold, $P_{abl} \approx 0.5$ GPa, is generated by roughly equal contributions from the shock and thermochemical decomposition. Ablation under these conditions can be described in terms of *shock-assisted photothermal ablation*. Pressure and temperature jumps as high as 2.5 GPa and 600 °C have been calculated from CARS measurements. The CARS measurements of PMMA ablation also showed a feature which was assigned to the monomer, MMA, an ablation product[105] which is expected for a thermal process associated with temperatures above the ceiling temperature (550 K) of PMMA.

Polymer ablation by ultrafast laser pulses is a relatively new field, with many open questions. In the case of fs pulses, the pronounced difference in the quality of features formed in PMMA by UV and near-IR lasers has not been explained.

 © 2005 WILEY-VCH Verlag GmbH & Co. KGaA, Weinheim

The nature of incubation and the mechanisms for microstructure formation, especially the differences for differently polarized beams, are interesting fields for future studies.

Vacuum-Ultraviolet (VUV) Lasers

In the case of polymers, VUV structuring provides an important alternative to fs laser ablation. The necessary laser wavelengths, e.g., at 157 nm (F_2 excimer) are already commercially available. Most materials are opaque in the VUV and the high photon energies (e.g., 7.9 eV at 157 nm) can break chemical bonds; this bond breaking ability should minimize thermal loading at the target surface. The sub-quarter-micron-features that can be produced with VUV lasers are not accessible at the fundamental of the Ti:sapphire laser. The disadvantages of VUV radiation include the necessity to perform irradiation in vacuum, or at least in inert gases. Furthermore, at 157 nm, fluoride-based optics (e.g., CaF_2 or MgF_2) are required.

The first reports of polymer ablation at 157-nm appeared in the mid-80's with a self-developing, i.e., direct ablation, nitrocellulose resist.[106] Subsequent work was used to characterize the ablation thresholds for a variety of polymers,[107] such as PET, PI (Kapton^{TM}), and PE. The resulting high quality structures showed no visible thermal damage. A more detailed study of PET, including analysis of the volatile ablation products, indicates that photochemical processes significantly contribute to ablation.[108] Various other studies supported a dominating photochemical mechanism.[5,109] F_2 excimer laser irradiation was applied to create a variety of complex microstructures in PMMA, PC and polystyrene (PS) using a silicone membrane contact mask[110] or microdroplets.[111]

A very different VUV irradiation source (125 nm) has been developed based on four-wave sum frequency mixing in Hg vapor at room temperature.[112,113] Threshold fluences for PMMA and PTFE under these conditions are about 1 $mJ \cdot cm^{-2}$, with corresponding ablation rates of 9.7 Å $pulse^{-1}$ for PMMA and 6.7 Å $pulse^{-1}$ for poly(tetrafluoroethylene) (PTFE). The extremely low threshold fluences and the ablation rates are much lower than the thermal diffusion lengths of 56 nm for PMMA and 76 nm for PTFE which are clear indications for a predominantly photochemical ablation mechanism.[114]

The experimental data on VUV polymer ablation strongly support the operation of photochemical ablation processes. Systematic studies of the ablation products and their temporal evolution and energies are required to determine the role of photothermal processes, if any. VUV ablation is an attractive alternative to ultrafast structuring, as the 157 nm laser system is quite simple.

Other Irradiation Sources

A wide variety of other irradiation sources has also been applied for polymer ablation, which are only discussed briefly here.

Synchrotron radiation yields very high aspect ratios and structuring is possible without defined threshold fluence with products that are different to those associated with thermal ablation, i.e., the main product of Teflon® structuring is CF_3^+ compared to C_2F_4 for laser ablation at 248 nm.[115–119]

Mid-IR irradiation is mainly performed by CO_2 lasers,[120–124] and very high ablation rates[125] and high quality structures may be obtained.[126] Alternatively CO[127] or mid-IR FEL have been employed for ablation.[128] The FEL was also used for polymer film deposition[129] where indications exist that the ablation behavior depends strongly on which functional group is excited.[130]

Visible[131] and *high repetition rate* lasers are rather seldom used for ablation studies, but the high repetition rate lasers (usually in the kHz range, but up to 20 kHz) have been used for drilling and wire stripping in the electronic industry for several years. The ablation studies proved that cumulative heating influences the ablation behavior, i.e., showing increasing ablation rates.[132,133]

Surface Modification of Polymers

Chemical surface modification during laser ablation strongly depends on whether the fluence is above or below the ablation threshold. Most experiments have focused on fluences above the threshold of ablation. Recently, reviews of polymer surface modification have appeared[134,135] and generally the following trends can be observed. Absorbing species are often produced during incubation. Incubation is either due to reactions between groups that have been activated by the laser photons within the polymer or between active groups and the ambient. The ambient could be air, supplied gases,[136,137] or supplied liquids.[138,139] Polymers containing aromatic groups (e.g., polyimide) are often carbonized at fluences above the ablation threshold of ablation.

Irradiation of polymer surfaces at fluences below the ablation threshold can be exploited to alter surface properties such as hydrophilicity, wettability, and adhesion. Polymer metallization[140] is one important technical process which is employed in microelectronics packaging and MCM (Multi Chip Module) technology, as well as in the production of decorative overlayers, diffusion barriers, and electromagnetic shielding. The state-of-the-art wet chemical metallization of polymers involves a pretreatment, i.e., cleaning, activation, and prenucleation, followed by metal deposition by laser-assisted processes, liquid phase deposition, or vacuum deposition.[141,142] Alternative pretreatment processes are plasma discharge and ion etching[143] and photochemical surface modification[144] which are typically dry processes that work well as pretreatment steps. Examples of photochemical modification performed with UV lasers are the 248 nm irradiation of poly(butylene terephthalate) (PBT)[145,146] and PI which results in the

© 2005 WILEY-VCH Verlag GmbH & Co. KGaA, Weinheim

loss of oxygen functionality (PI also loses nitrogen functionality) but also an improvement of the adhesion of subsequently deposited metal films is obtained. Other examples are the 193 nm irradiation of PI which was utilized to selectively deposit copper on PI by electroless plating;[147] the treatment of PET which improves the metallization by thermally evaporated Al;[148] the laser-induced surface cleaning, amorphization, and chemical modification of poly(ether ether ketone) (PEEK) which improves the adhesive bonding properties;[149] and the UV treatment of fibers, which have been employed to improve rubber-fiber adhesion.[150]

An interesting variation of polymer surface modification is the utilization of reactive species created by irradiation of a frozen azide (pentafluorophenyl azide) at 248 nm in vacuum which has been utilized to increase the nitrogen and fluorine content of PET.[151,152]

Modifications of polymers surfaces are of course possible with lasers, but commercial applications are hindered by the high cost of laser photons. In many cases, low intensity UV and VUV lamps can modify large areas at considerably lower photon costs. Low intensity lamps include mercury lamps at 185 nm, Xe (147 nm) and Kr (123.6 nm) resonance lamps, He discharge lamps with $\lambda < 160$ nm, and excimer lamps at 126 (Ar_2), 146 (Kr_2), 172 (Xe_2), 222 (KrCl), and 308 (XeCl) nm. Under well-controlled conditions, even polymer etching has been achieved with mercury lamps, excimer lamps, and discharge lamps. VUV sources such as cold plasmas[153–155] and VUV resonance lamps[156,157] have also been applied to study the transformation and degradation of organic polymers or to improve micro wear resistance.[157] The VUV irradiation of cold plasmas has also been used to simulate certain conditions in outer space to test long-term stability of materials under these conditions.[158,159]

Surface modification of PMMA, PI, and PET has been studied in detail for 185 nm irradiation. An increase of the O/C ratio (surface oxidation) was determined by XPS measurements for irradiation in air[160,161] while a decrease in the O/C ratio was detected for irradiation in vacuum.[162] The decrease of oxygen in the surface of the film was attributed to the loss of small gaseous molecules, such as CO and CO_2. Conversely, surface oxidation was attributed to the reaction of surface carbon radicals with atmospheric oxygen.

Xe resonance lamps (147 nm) have been used to increase the surface polarity of a variety of very unpolar polymers, including siloxanes and FEP. An increase of CO and OH functionalities is observed after irradiation.[157,163,164]

More commonly excimer lamps have been used to modify polymer surfaces, e.g., fluoropolymers.[165,166] Surface roughening is often observed[167] and in the presence of appropriate oxygen concentrations even etching with excimer lamps can be achieved with much higher (factor 40 to 100)[168] etch rates than for Hg lamps (etch rates around 50 Å min^{-1}).[169,170] For PI (Kapton™) and PMMA irradiated at 172 and 222 nm, the optimum oxygen pressure is about 1 mbar. The etching mechanism has been described as *photo-oxidative etching*, where irradiation produces reactive oxygen species such as free radicals [$O(^1D)$, $O(^3P)$] and excited molecular oxygen. Etching is obtained when these reactive species oxidize the surface to form gaseous products, e.g., CO and CO_2. Excimer lamps have also been used to etch various acrylates in high vacuum (<0.03 Torr). The degradation efficiency depends on the structure of the ester side chain. Polymers with low T_g were easily decomposed especially during irradiation at elevated temperatures (50 to 130 °C).[171]

Recently excimer lamps have been used to modify an important technical polymer i.e., polydimethylsiloxane (PDMS, general structure shown in Figure 25).[172–174] PDMSs are widely used as coatings in a variety of fields including biomedical applications, such as membrane technology, microlithography, optics and dielectrics.[175,176]

Cross-linked poly(siloxane)s possess unique mechanical, nearly ideal elastomer and optical properties, low weight, high durability, high gas permeability and excellent water repellency.[177,178] The modification of the hydrophobic PDMS to hydrophilic SiO_x opens an additional wide range of applications i.e., in microelectronics[179–181] and coating technology for medical devices.[182–184] Transformation of PDMS into a SiO_x structure has been achieved by irradiation with a Xe_2 excimer lamp at 172 nm in air.[172–174] The modification of the surface properties have been analyzed in detail by contact angle measurements of water, which reveal a fast decrease of the contact angle as a function of irradiation time and intensity (shown in Figure 26). This change of the contact angle is associated with a change of the chemical composition of the surface, which has been measured by XPS.[172] The surface layer becomes enriched in oxygen and depleted in carbon to reach an O/Si ratio of almost 2 (shown in Figure 27). This corresponds almost to the "ideal" composition of SiO_2 which is also confirmed by determining the refractive index, n, by spectroscopic ellipsometry.[174] The value of n increases with irradiation time and reaches almost the literature value for SiO_2 (shown in Figure 28) of 1.457.[185] The chemical composition has also been confirmed by Energy Dispersive X-ray Spectroscopy, where a value of 1.94 for the O/Si ratio was obtained. High resolution Transmission Electron Microscopy (TEM) cross-section (Figure 29) shows the homogeneous layer of SiO_x formed by irradiation of the PDMS. The SiO_x layer is

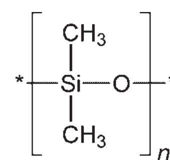

Figure 25. Chemical structure of PDMS.

© 2005 WILEY-VCH Verlag GmbH & Co. KGaA, Weinheim

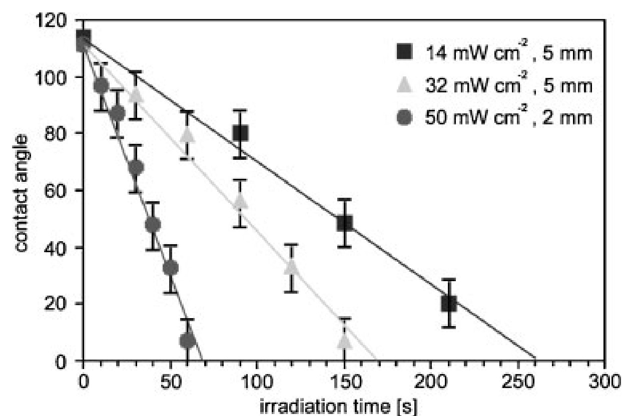

Figure 26. Water contact angles on PDMS for 172 nm irradiation in air for various irradiation times and intensities.

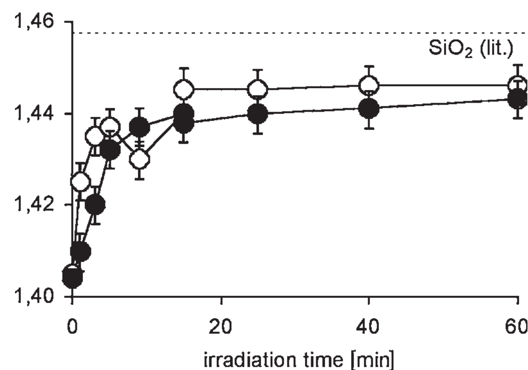

Figure 28. Refractive index as function of the irradiation time as obtained by spectroscopic ellipsometry. Layer thicknesses prior to irradiation: ○ 118 nm, ● 232 nm.

on top of the native SiO_2 layer of the Si substrate. It appears that the complete layer (192 nm) of PDMS has been transformed to SiO_x which implies that the reactive oxygen species diffuse through the modified PDMS layer. The mechanism of the PDMS oxidation has been studied using Attenuated Total Reflection (ATR) FT-IR measurements,[172] and a complex mechanisms has been suggested (Figure 30, where the detected intermediates are marked).

The initial step is bond breaking either in the main chain (Si–O) or in the side groups of the polymer (Si–C and C–H). Further reactions of the silicon and methylene radicals with oxygen lead to the formation of peroxy radicals which rearrange to give silanol groups. The oxygen radical can attack a Si–C bond to create a new Si–O–Si bridge which can also be formed between polymer chains, resulting in crosslinking. The silicon radical can also react with a hydroxyl radical, which is formed by the absorption of 172 nm in air, to form a silanol group (Si–OH). The formation of stable intermediates including methylene groups was not verified but the formation of carbonyl groups during irradiation was detected.

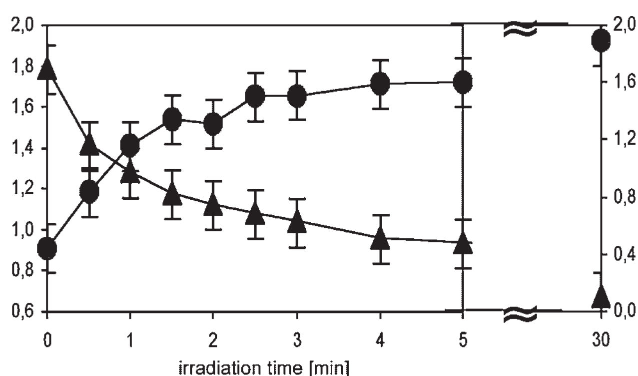

Figure 27. Changes of the O/Si (●) and C/Si (▲) atomic ratios of PDMS exposed to 172 nm (16.6 mW · cm^{-2}) irradiation in air with various irradiation times as determined by XPS.

Another direction of surface modification of polymers is the incorporation of other functional groups into polymers, such as nitrogen in the form of amino groups which allow another class of reactions to further modify the polymer surface. Surface modifications have been achieved for various polyolefines, such as polyethylene and poly(propylene) (PP) using a Kr resonance lamp which emits at 123.6 nm and a D_2Ar continuum lamp that emits between 110–170 nm.[186,187] Irradiations was carried out in the presence of NH_3 which absorbs strongly in the 112 nm to 220 nm range, while the polymers only absorb at wavelengths below 170 nm. In both cases a pronounced incorporation of nitrogen has been achieved, with a higher nitrogen content of up to 25% for the Kr-lamp irradiation.

A Xe_2 excimer lamp has also been tested, but no incorporation of nitrogen was detected, suggesting that the modification of the polymer surface is depending on the activation of ammonia to form reactive species, such as amino and imino radicals in the ground or excited state, as well as on the direct activation of the polymer by the VUV photons.

It is worth mentioning that in the case of oxidized PDMS as well as for the nitriding of the polyolefins a surface reconstruction or recovery occurs. This has been assigned for PDMS to a migration of bulk PDMS or monomers to the surface.[172] For the polyolefins a rotational and/or translational motion of the polymer chains result in hydrophobic layers (1 nm) while the reaction of long-lived radicals with water or oxygen have been observed in deeper layers (10 nm). It was also possible to reduce these reactions by cross-linking near the surface.[187]

Different etching processes are active for irradiation with Kr_2 excimer lamps at 146 nm[188] and He discharge lamps (<160 nm)[189] in N_2, He, or H_2 atmospheres. Irradiation at 146 nm can be applied to etch PMMA and other polyacrylates, but not PS. Poly(phenylquinoxaline) (PPQ) is etched with He discharge radiation, with the C–H bond as a possible initial decomposition site.

© 2005 WILEY-VCH Verlag GmbH & Co. KGaA, Weinheim

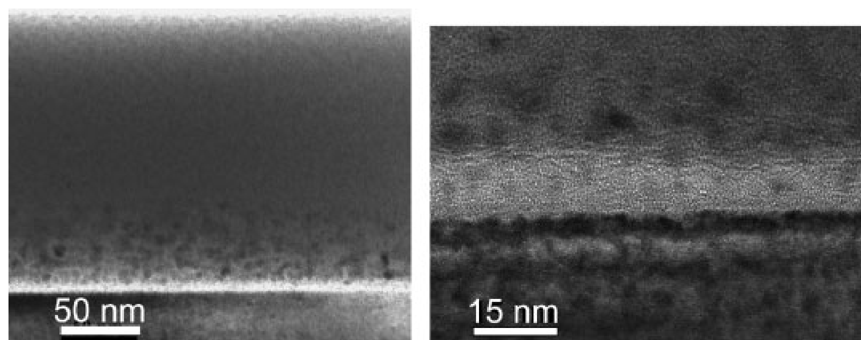

Figure 29. TEM crosssections of a PDMS film on a Si substrate after 40 min irradiation at 172 nm in air. The Si substrate is on the bottom of the pictures followed by the "white" SiO_2 layer and the modified PDMS film. The O/Si ratio of the modified PDMS film, determined by Energy Dispersive X-ray Spectroscopy, is 1.94.

Conclusion

Laser ablation of polymers is an established technique in various industrial applications and the large number of studies published annually indicate that this is still an attractive area of research. Discussions about the ablation mechanisms are ongoing and will remain one of the topics in ablation of polymers. The development of polymers specifically designed for laser ablation is a unique tool for probing the ablation mechanisms as well as for improving ablation properties. New commercial applications will require improved ablation rates and control of undesirable surface effects, such as debris. The complexity of interactions between polymers and laser photons are illustrated by the various processes associated with different irradiation conditions, i.e., the photokinetic etching with CW UV lasers, the probably purely photochemical ablation for VUV lasers, the mixed photothermal-photochemical laser ablation for other irradiation wavelengths, the shock-assisted photothermal ablation on ps time scales, the

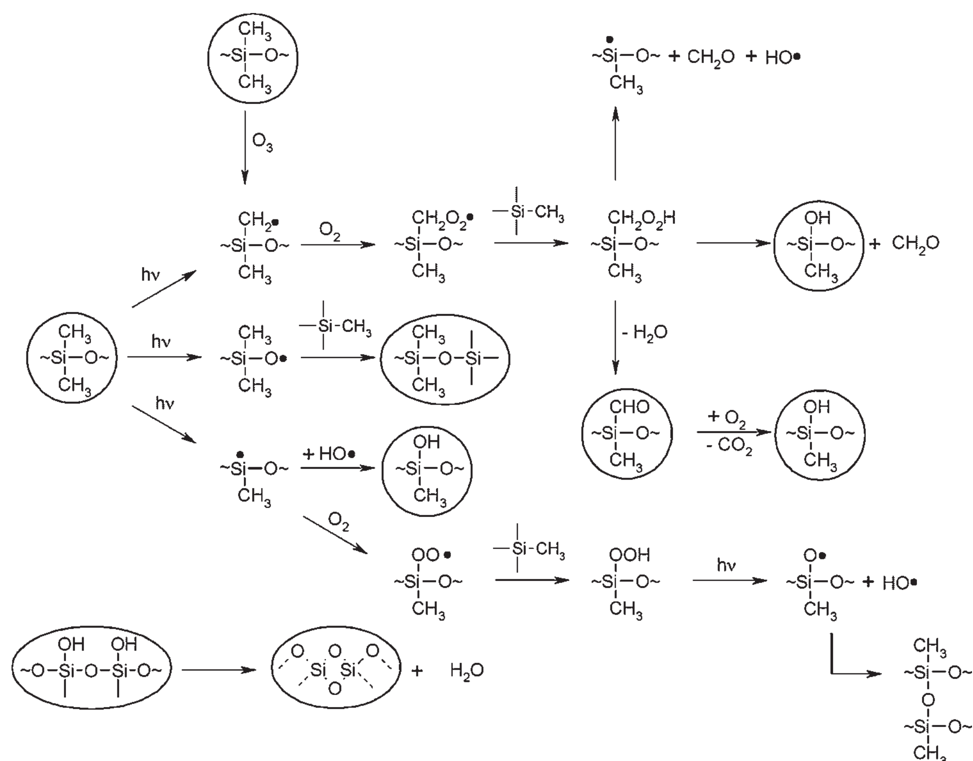

Figure 30. Survey of possible reactions involved in the oxidation process of PDMS during irradiation at 172 nm in air. The framed structures have been detected by ATR-FTIR measurements.

 © 2005 WILEY-VCH Verlag GmbH & Co. KGaA, Weinheim

wavelength and polarization dependent ablation with fs-lasers, the influence of exciting various functional groups for mid-IR ablation and the completely different etching mechanisms for synchrotron structuring.

The ongoing maturation of laser techniques will increase the number of applications of laser ablation in the future. In the last decade we have seen the development of several exciting laser ablation tools, including fs lasers, VUV lasers, FELs, and high repetition-rate lasers. All these new techniques are applied in ongoing research in conjunction with a variety of analytical techniques. Femtosecond lasers and VUV lasers in particular are expected to lead to important industrial applications.

The simultaneous development of various VUV sources for large area irradiation, such as excimer or resonance lamps, will also result in a steady increase of applications and a better understanding of photon-induced processes in polymers. While surface oxidation of selected polymers with 172 nm irradiation in air and the nitriding in the presence of ammonia using 123.6 nm seems reasonably well understood, etching in non-oxidizing atmosphere is certainly not. The photochemistry using VUV radiation will also be an attractive research area in the future, especially with the ongoing decrease of the irradiation wavelengths in lithography.

Acknowledgements: This work has been partially supported by the *Swiss National Science Foundation*. I would also like to thank *Cosmin Sandu* for the TEM analysis and Dr. *V.-M. Graubner* and *L. Urech* for their assistance and various data.

[1] R. Srinivasan, S. Mayne-Banton, *Appl. Phys. Lett.* **1982**, *41*, 576.
[2] Y. Kawamura, K. Toyoda, S. Namba, *Appl. Phys. Lett.* **1982**, *40*, 374.
[3] R. Srinivasan, B. Braren, *Chem. Rev.* **1989**, *89*, 1303.
[4] P. E. Dyer, ‘‘*Photochemical Processing of Materials*’’, Academic Press, London 1992.
[5] S. Lazare, V. Granier, *Laser Chem.* **1989**, *10*, 25.
[6] D. Bäuerle, ‘‘*Laser Processing and Chemistry*’’, 3rd edition, Springer, Berlin, New Nork 2000.
[7] T. Lippert, J. T. Dickinson, *Chem. Rev.* **2003**, *103*, 453.
[8] T. Lippert, *Adv. Polym. Sci.* **2004**, *168*, 51.
[9] N. Arnold, N. Bityurin, *Appl. Phys. A* **1999**, *68*, 615.
[10] N. Bityurin, B. S. Luk'yanchuk, M. H. Hong, T. C. Chong, *Chem. Rev.* **2003**, *103*, 519.
[11] J. F. Rabek, ‘‘*Mechanism of Photophysical Processes and Photochemical Reactions in Polymers*’’, J. Wiley & Sons, New York 1987.
[12] D. B. Chrisey, A. Pique, R. A. McGill, J. S. Horwitz, B. R. Ringeisen, D. M. Bubb, P. K. Wu, *Chem. Rev.* **2003**, *103*, 553.
[13] A. Pique, R. A. McGill, D. B. Chrisey, D. Leonhardt, T. E. Mslna, B. J. Spargo, J. H. Callahan, R. W. Vachet, R. Chung, M. A. Bucaro, *Thin Solid Films* **1999**, *356*, 536.
[14] B. Toftmann, M. R. Papantonakis, R. C. Y. Auyeung, W. Kim, S. M. O'Malley, D. M. Bubb, J. S. Horwitz, J. Schou, P. M. Johansen, R. E. Haglund, *Thin Solid Films* **2004**, *453–454*, 177.
[15] R. S. Patel, T. A. Wassick, *Proc. SPIE – Int. Soc. Opt. Eng.* **1997**, *2991*, 217.
[16] US 5736999 (1998), inv.: H. Aoki.
[17] R. Srinivasan, B. Braren, D. E. Seeger, R. W. Dreyfus, *Macromolecules* **1986**, *19*, 916.
[18] R. Srinivasan, *J. Appl. Phys.* **1993**, *73*, 2743.
[19] T. Lippert, R. L. Webb, S. C. Langford, J. T. Dickinson, *J. Appl. Phys.* **1999**, *85*, 1838.
[20] M. Hertzberg, I. A. Zlochower, *Combust. Flame* **1991**, *84*, 15.
[21] A. K. Baker, P. E. Dyer, *Appl. Phys. A* **1993**, *57*, 543.
[22] C. Wochnowski, M. Koerdt, S. Metev, F. Vollertsen, in: *Fifth International Symposium on Laser Precision Microfabrication*, Vol. 5662, I. Miyamoto, H. Helvajian, K. Itho, K. F. Kobayashi, A. Ostendorf, K. Sugioka, Eds., SPIE, Nara, Japan 2004, p. 232.
[23] C. Wochnowski, R. Meteva, S. Metev, in: *Laser Precision Microfabrication*, Vol. 4830, SPIE, Osaka, Japan 2003, p. 396.
[24] J. Y. Cheng, C. W. Wei, K. H. Hsu, T. H. Young, *Sens. Actuators, B* **2004**, *99*, 186.
[25] T. Lippert, A. Yabe, A. Wokaun, *Adv. Mater.* **1997**, *9*, 105.
[26] H. Fukumura, H. Masuhara, *Chem. Phys. Lett.* **1994**, *221*, 373.
[27] T. Lippert, J. Stebani, O. Nuyken, A. Stasko, A. Wokaun, *J. Photochem. Photobiol., A* **1994**, *78*, 139.
[28] O. Nuyken, J. Stebani, T. Lippert, A. Wokaun, A. Stasko, *Macromol. Chem. Phys.* **1995**, *196*, 751.
[29] A. Stasko, V. Adamcik, T. Lippert, A. Wokaun, J. Dauth, O. Nuyken, *Makromol. Chem.* **1993**, *194*, 3385.
[30] T. Lippert, A. Wokaun, J. Stebani, O. Nuyken, J. Ihlemann, *Angew. Makromol. Chem.* **1993**, *213*, 127.
[31] O. Nuyken, J. Stebani, T. Lippert, A. Wokaun, A. Stasko, *Macromol. Chem. Phys.* **1995**, *196*, 739.
[32] T. Lippert, L. S. Bennett, T. Nakamura, H. Niino, A. Ouchi, A. Yabe, *Appl. Phys. A* **1996**, *63*, 257.
[33] T. Lippert, A. Wokaun, J. Stebani, O. Nuyken, J. Ihlemann, *Angew. Makromol. Chem.* **1993**, *206*, 97.
[34] T. Lippert, J. Stebani, J. Ihlemann, O. Nuyken, A. Wokaun, *J. Phys. Chem.* **1993**, *97*, 12296.
[35] T. Lippert, T. Nakamura, H. Niino, A. Yabe, *Macromolecules* **1996**, *29*, 6301.
[36] T. Lippert, T. Nakamura, H. Niino, A. Yabe, *Appl. Surf. Sci.* **1997**, *110*, 227.
[37] T. Lippert, E. Ortelli, J. C. Panitz, F. Raimondi, J. Wambach, J. Wei, A. Wokaun, *Appl. Phys. A* **1999**, *69*, S651.
[38] F. Raimondi, S. Abolhassani, R. Brutsch, F. Geiger, T. Lippert, J. Wambach, J. Wei, A. Wokaun, *J. Appl. Phys.* **2000**, *88*, 3659.
[39] P. E. Dyer, D. M. Karnakis, G. A. Oldershaw, G. C. Roberts, *J. Phys. D: Appl. Phys.* **1996**, *29*, 2554.
[40] P. E. Dyer, I. Waldeck, G. C. Roberts, *J. Phys. D: Appl. Phys.* **1997**, *30*, L19.
[41] T. Masabuchi, T. Tada, E. Nomura, K. Hatanaka, H. Fukumura, H. Masuhara, *J. Phys. Chem. A* **2002**, *106*, 2180.
[42] T. Lippert, C. David, M. Hauer, T. Masabuchi, H. Masuhara, E. Nomura, O. Nuyken, C. Phipps, J. Robert, T. Tada, K. Tomita, A. Wokaun, *Appl. Surf. Sci.* **2002**, *186*, 14.
[43] S. Küper, J. Brannon, K. Brannon, *Appl. Phys. A* **1993**, *56*, 43.

© 2005 WILEY-VCH Verlag GmbH & Co. KGaA, Weinheim

[44] J. E. Andrews, P. E. Dyer, D. Forster, P. H. Key, *Appl. Phys. Lett.* **1983**, *43*, 717.
[45] R. Srinivasan, B. Braren, *J. Polym. Sci., Part A: Polym. Chem.* **1984**, *22*, 2601.
[46] M. Schumann, R. Sauerbrey, M. Smayling, *Appl. Phys. Lett.* **1991**, *58*, 428.
[47] T. Feurer, R. Sauerbrey, M. C. Smayling, B. J. Story, *Appl. Phys. A* **1993**, *56*, 275.
[48] Z. Ball, T. Feurer, D. L. Callahan, R. Sauerbrey, *Appl. Phys. A* **1996**, *62*, 203.
[49] T. Dumont, S. Lazare, T. Lippert, A. Wokaun, *Appl. Phys. A* **2004**, *79*, 1271.
[50] J. Wei, N. Hoogen, T. Lippert, O. Nuyken, A. Wokaun, *J. Phys. Chem. B* **2001**, *105*, 1267.
[51] T. Lippert, J. Wei, A. Wokaun, N. Hoogen, O. Nuyken, *Appl. Surf. Sci.* **2000**, *168*, 270.
[52] T. Lippert, J. Wei, A. Wokaun, N. Hoogen, O. Nuyken, *Macromol. Mater. Eng.* **2000**, *283*, 140.
[53] J. Wei, N. Hoogen, T. Lippert, C. Hahn, O. Nuyken, A. Wokaun, *Appl. Phys. A* **1999**, *69*, S849.
[54] T. Lippert, C. David, J. T. Dickinson, M. Hauer, U. Kogelschatz, S. C. Langford, O. Nuyken, C. Phipps, J. Robert, A. Wokaun, *J. Photochem. Photobiol. A* **2001**, *145*, 145.
[55] T. Lippert, L. S. Bennett, T. Nakamura, H. Niino, A. Yabe, *Appl. Surf. Sci.* **1996**, *96–98*, 601.
[56] H. Fukumura, E.-I. Takahashi, H. Masuhara, *J. Phys. Chem.* **1995**, *99*, 750.
[57] R. Srinivasan, K. G. Casey, B. Braren, M. Yeh, *J. Appl. Phys.* **1990**, *67*, 1604.
[58] H. Furutani, H. Fukumura, H. Masuhara, *J. Phys. Chem.* **1996**, *100*, 6871.
[59] H. Kim, J. C. Postlewaite, T. Zyung, D. D. Dlott, *J. Appl. Phys.* **1988**, *64*, 2955.
[60] M. Hauer, D. J. Funk, T. Lippert, A. Wokaun, *Opt. Laser Eng.* **2005**, *43*, 545.
[61] L. S. Bennett, T. Lippert, H. Furutani, H. Fukumura, H. Masuhara, *Appl. Phys. A* **1996**, *63*, 327.
[62] M. Hauer, D. J. Funk, T. Lippert, A. Wokaun, *Appl. Phys. A* **2003**, *77*, 297.
[63] H. Furutani, H. Fukumura, H. Masuhara, *Appl. Phys. Lett.* **1994**, *65*, 3413.
[64] H. Furutani, H. Fukumura, H. Masuhara, T. Lippert, A. Yabe, *J. Phys. Chem. A* **1997**, *101*, 5742.
[65] M. Hauer, D. J. Funk, T. Lippert, A. Wokaun, *Proc. SPIE – Int. Soc. Opt. Eng.* **2002**, *4760*, 259.
[66] T. Lippert, A. Wokaun, S. C. Langford, J. T. Dickinson, *Appl. Phys. A* **1999**, *69*, S655.
[67] T. Lippert, S. C. Langford, A. Wokaun, S. Georgiou, J. T. Dickinson, *J. Appl. Phys.* **1999**, *86*, 7116.
[68] O. Nuyken, J. Stebani, T. Lippert, A. Wokaun, A. Stasko, *Macromol. Chem. Phys.* **1995**, *196*, 751.
[69] S. C. Langford, J. T. Dickinson, M. Hauer, T. Lippert, A. Wokaun, submitted.
[70] J. T. Dickinson, J.-J. Shin, W. Jiang, M. G. Norton, *J. Appl. Phys.* **1993**, *74*, 4729.
[71] M. Himmelbauer, E. Arenholz, D. Bäuerle, *Appl. Phys. A* **1996**, *63*, 87.
[72] M. Himmelbauer, E. Arenholz, D. Bäuerle, K. Schilcher, *Appl. Phys. A* **1996**, *63*, 337.
[73] D. Bäuerle, M. Himmelbauer, E. Arenholz, *J. Photochem. Photobiol. A* **1997**, *106*, 27.
[74] K. Piglmayer, E. Arenholz, C. Ortwein, N. Arnold, D. Bäuerle, *Appl. Phys. Lett.* **1998**, *73*, 847.
[75] R. Srinivasan, *Appl. Phys. Lett.* **1991**, *58*, 2895.
[76] R. Srinivasan, *J. Appl. Phys.* **1992**, *72*, 1651.
[77] R. Srinivasan, R. R. Hall, W. D. Loehle, W. D. Wilson, D. C. Allbee, *J. Appl. Phys.* **1995**, *78*, 4881.
[78] J. D. Bonlie, F. Patterson, D. Price, B. White, P. Springer, *Appl. Phys. B* **2000**, *70*, S155.
[79] R. Haight, D. Hayden, P. Longo, T. Neary, A. Wagner, *Proc. SPIE – Int. Soc. Opt. Eng.* **1998**, *3546*, 477.
[80] Y. Shani, I. Melnick, S. Yoffe, Y. Sharon, K. Lieberman, H. Terkel, *Proc. SPIE – Int. Soc. Opt. Eng.* **1998**, *3546*, 112.
[81] R. Srinivasan, E. Sutcliffe, B. Braren, *Appl. Phys. Lett.* **1987**, *51*, 1285.
[82] S. Küper, M. Stuke, *Appl. Phys. B* **1987**, *44*, 199.
[83] J. Kruger, W. Kautek, *Adv. Polym. Sci.* **2004**, *168*, 247.
[84] S. Küper, M. Stuke, *Appl. Phys. Lett.* **1989**, *54*, 4.
[85] S. Küper, M. Stuke, *Mater. Res. Soc. Symp. Proc.* **1989**, *129*, 375.
[86] H. Kumagai, K. Midorikawa, K. Toyoda, S. Nakamura, T. Okamoto, M. Obara, *Appl. Phys. Lett.* **1994**, *65*, 1850.
[87] S. Baudach, J. Bonse, W. Kautek, *Appl. Phys. A* **1999**, *69*, S395.
[88] S. Baudach, J. Bonse, J. Krüger, W. Kautek, *Appl. Surf. Sci.* **2000**, *154–155*, 555.
[89] J. Bonse, S. Baudach, J. Krüger, W. Kautek, *Proc. SPIE – Int. Soc. Opt. Eng.* **2000**, *4065*, 161.
[90] S. Baudach, J. Krüger, W. Kautek, *Rev. Laser Eng.* **2001**, *29*, 705.
[91] K. Yamasaki, S. Juodkazis, T. Lippert, M. Watanabe, S. Matsuo, H. Misawa, *Appl. Phys. A* **2003**, *76*, 325.
[92] B. Hopp, Z. Toth, K. Gal, A. Mechler, Z. Bor, S. D. Moustaizis, S. Georgiou, C. Fotakis, *Appl. Phys. A* **1999**, *69*, S191.
[93] Z. Toth, B. Hopp, A. Mechler, Z. Bor, S. D. Moustaizis, A. Athanassiou, S. Georgiou, C. Kalpouzos, C. Fotakis, *Laser Phys.* **2000**, *10*, 241.
[94] J. Bonse, S. M. Wiggins, J. Solis, T. Lippert, *Appl. Surf. Sci.* **2005**, *241*, 440.
[95] J. Bonse, S. M. Wiggins, J. Solis, T. Lippert, H. Sturm, *Appl. Surf. Sci.* **2005**, *248*, 157.
[96] C. Hahn, T. Lippert, A. Wokaun, *J. Phys. Chem. B* **1999**, *103*, 1287.
[97] X. Wen, W. Tolbert, D. D. Dlott, *Chem. Phys. Lett.* **1992**, *192*, 315.
[98] H. Fujiwara, H. Fukumura, H. Masuhara, *J. Phys. Chem.* **1995**, *99*, 11844.
[99] H. Kim, J. C. Postlewaite, T. Zhung, D. D. Dlott, *Appl. Phys. Lett.* **1989**, *54*, 2274.
[100] T. Zhung, H. Kim, J. C. Postlewaite, D. D. Dlott, *J. Appl. Phys.* **1989**, *65*, 4548.
[101] X. Wen, D. E. Hare, D. D. Dlott, *Appl. Phys. Lett.* **1994**, *64*, 184.
[102] D. E. Hare, J. Franken, D. D. Dlott, E. L. Chronister, J. J. Flores, *Appl. Phys. Lett.* **1994**, *65*, 3051.
[103] D. E. Hare, J. Franken, D. D. Dlott, *J. Appl. Phys.* **1995**, *77*, 5950.
[104] I.-Y. Sandy Lee, X. Wen, W. A. Tolbert, D. D. Dlott, M. Doxtader, D. R. Arnold, *J. Appl. Phys.* **1992**, *72*, 2440.
[105] D. E. Hare, D. D. Dlott, *Appl. Phys. Lett.* **1994**, *64*, 715.
[106] D. Henderson, J. C. White, H. G. Craighead, I. Adesida, *Appl. Phys. Lett.* **1985**, *45*, 900.
[107] P. E. Dyer, J. Sidhu, *J. Opt. Soc. Am. B* **1986**, *3*, 792.
[108] P. E. Dyer, G. A. Oldershaw, D. Schudel, *J. Phys. D: Appl. Phys.* **1992**, *25*, 323.
[109] S. Lazare, V. Granier, *J. Appl. Phys.* **1988**, *63*, 2110.
[110] M. Lapczyna, M. Stuke, *Mater. Res. Soc. Proc.* **1998**, *526*, 143.

 © 2005 WILEY-VCH Verlag GmbH & Co. KGaA, Weinheim

[111] M. Lapczyna, M. Stuke, *Appl. Phys. A* **1998**, *66*, 473.
[112] L. Museur, W. Q. Zheng, A. V. Kanaev, M. C. Castex, *IEEE J. Quantum Electron.* **1995**, *1*, 900.
[113] D. Riedel, M. C. Castex, *Proc. SPIE – Int. Soc. Opt. Eng.* **1998**, *3404*, 234.
[114] D. Riedel, M. C. Castex, *Appl. Phys. A* **1999**, *69*, 375.
[115] T. Katoh, Y. Zhang, *J. Synchroton Radiat.* **1998**, *5*, 1153.
[116] T. Katoh, D. Yamaguchi, Y. Satoh, S. Ikeda, Y. Aoki, M. Washio, Y. Tabata, *Appl. Surf. Sci.* **2002**, *186*, 24.
[117] Y. Zhang, T. Hori, *Synchrotron Radiat. News* **2000**, *13*, 32.
[118] Y. Zhang, T. Katoh, M. Washio, H. Yamada, S. Hamada, *Appl. Phys. Lett.* **1995**, *67*, 872.
[119] Y. Zhang, *Adv. Polym. Sci.* **2004**, *168*, 291.
[120] R. F. Cozzens, R. B. Fox, *Polym. Eng. Sci.* **1978**, *18*, 900.
[121] G. Koren, *Appl. Phys. Lett.* **1984**, *45*, 10.
[122] J. H. Brannon, J. R. Lankard, *Appl. Phys. Lett.* **1986**, *48*, 1226.
[123] R. Braun, R. Nowak, P. Hess, H. Oetzmann, C. Schmidt, *Appl. Surf. Sci.* **1989**, *43*, 352.
[124] M. F. Sonnenschein, C. M. Roland, *Appl. Phys. Lett.* **1990**, *57*, 425.
[125] T. Sumiyoshi, Y. Ninomiya, H . Ogasawara, M. Obara, H. Tanaka, *Appl. Phys. A* **1994**, *58*, 475.
[126] P. E. Dyer, D. M. Karnakis, G. A. Oldershaw, G. C. Roberts, *J. Appl. Phys. D: Appl. Phys.* **1996**, *26*, 2554.
[127] A. Ionin, Y. Klimachev, H. Kobsa, D. Sinistyn, *Proc. SPIE – Int. Soc. Opt. Eng.* **1998**, *3343*, 1032.
[128] M. J. Kelly, *Mater. Res. Soc. Symp. Proc.* **2001**, *617*, J5.7.
[129] D. M. Bubb, B. Toftmann, R. F. Haglund, Jr., J. S. Horowitz, M. R. Papantonakis, R. A. McGill, P. W. Wu, D. B. Chrisey, *Appl. Phys. A* **2002**, *74*, 123.
[130] D. M. Bubb, M. R. Papantonakis, B. Toftmann, J. S. Horowitz, R. A. McGill, D. B. Chrisey, R. F. Haglund, Jr., *J. Appl. Phys.* **2002**, *91*, 9809.
[131] M. S. Silverstein, I. Visoly, O. Kesler, M. Janai, Y. Cassuto, *J. Vac. Sci. Technol. B* **1998**, *16*, 2957.
[132] E. K. Illy, D. J. W. Brown, M. J. Withford, J. A. Piper, *IEEE J. Quantum Electron.* **1999**, *5*, 1543.
[133] A. C. J. Glover, E. K. Illy, J. A. Piper, *IEEE J. Quantum Electron.* **1995**, *1*, 830.
[134] S. Lazare, P. Benet, W. Guan, M. Bolle, S. Mihailov, "*Excimer Lasers*", Kluwer Academic Publishers, Dordrecht 1994, p. 201.
[135] C.-M. Chan, T.-M. Ko, H. Hiraoka, *Surf. Sci. Rep.* **1996**, *24*, 1.
[136] H. Niino, A. Yabe, *Appl. Phys. Lett.* **1993**, *63*, 3527.
[137] H. Niino, H. Okano, K. Inui, A. Yabe, *Appl. Surf. Sci.* **1997**, *109–110*, 259.
[138] M. Okoshi, M. Murahara, K. Toyoda, *J. Mater. Res.* **1992**, *7*, 1912.
[139] M. Murahara, K. Toyoda, *J. Adhes. Sci. Technol.* **1995**, *9*, 1601.
[140] L. J. Gerenser, "*Metallization of Polymers*", Am. Chem. Soc., Washington, DC 1990.
[141] D. J. Ehrlich, J. Y. Tsao, "*Laser Microfabrication: Thin Film Processes and Lithography*", Academic Press, San Diego, CA, London 1989.
[142] A. Bauer, J. Ganz, K. Hesse, E. Koehler, *Appl. Surf. Sci.* **1990**, *46*, 113.
[143] G. Liebel, *Galvanotechnik* **1988**, *79*, 2883.
[144] H. Hiraoka, S. Lazare, *Appl. Surf. Sci.* **1990**, *46*, 246.
[145] D. A. Wesner, R. Weichenhain, W. Pfleging, H. Horn, E. W. Kreutz, *Fresenius' J. Anal. Chem.* **1997**, *358*, 248.
[146] H. Horn, S. Beil, D. A. Wesner, R. Weichenhein, E. W. Kreutz, *Nucl. Instrum. Methods Phys. Res., Sect. B* **1999**, *151*, 279.
[147] G. Zhao, H. M. Philips, H. Zheng, S. Tam, W. Li, G. Wen, Z. Gong, Y. Lam, *Proc. SPIE – Int. Soc. Opt. Eng.* **2000**, *3933*, 505.
[148] S. Petit, P. Laurens, J. Amouroux, F. Arefi-Khonsari, *Appl. Surf. Sci.* **2000**, *168*, 300.
[149] P. Laurens, B. Sadras, F. Decobert, F. Arefi-Khonsari, J. Amouroux, *Int. J. Adhes. Adhes.* **1998**, *18*, 19.
[150] H. Watanabe, T. Takata, *Angew. Makromol. Chem.* **1996**, *235*, 95.
[151] H. Niino, A. Yabe, *Appl. Surf. Sci.* **1996**, *96–98*, 572.
[152] H. Niino, A. Yabe, *J. Photochem. Photobiol. A* **1997**, *106*, 9.
[153] A. C. Fozza, J. Roch, J. E. Klemberg-Sapieha, A. Kruse, A. Holländer, M. R. Wertheimer, *Nucl. Instrum. Methods Phys. Res., Sect. B* **1997**, *131*, 205.
[154] A. Holländer, J. E. Klemberg-Sapieha, M. R. Wertheimer, *J. Polym. Sci., Part A: Polym. Chem.* **1996**, *34*, 1511.
[155] A. Holländer, J. E. Klemberg-Sapieha, M. R. Wertheimer, *J. Polym. Sci., Part A: Polym. Chem.* **1995**, *33*, 2013.
[156] V. E. Skurat, Y. I. Dorofeev, *Angew. Makromol. Chem.* **1994**, *216*, 205.
[157] V. N. Vasilets, K. Nakamura, Y. Uyama, S. Ogata, Y. Ikada, *Polymer* **1998**, *39*, 2875.
[158] M. A. Golub, *Makromol. Chem., Macromol. Symp.* **1992**, *53*, 379.
[159] D. G. Zimcik, M. R. Wertheimer, K. B. Balmain, R. C. Tennyson, *J. Spacecraft Rockets* **1991**, *28*, 652.
[160] R. Srinivasan, S. Lazare, *Polymer* **1985**, *26*, 1297.
[161] S. Lazare, P. D. Hoh, J. M. Baker, R. Srinivasan, *J. Am. Chem. Soc.* **1984**, *106*, 4288.
[162] R. Srinivasan, S. Lazare, *J. Phys. Chem.* **1986**, *90*, 2124.
[163] V. N. Vasilets, T. I. Yuranova, A. N. Ponomarev, *J. Photopolym. Sci. Technol.* **1994**, *7*, 309.
[164] V. N. Vasilets, I. Hirata, H. Iwata, Y. Ikada, *J. Polym. Sci., Part A: Polym. Chem.* **1998**, *36*, 2215.
[165] J. Heitz, H. Niino, A. Yabe, *Appl. Phys. Lett.* **1996**, *68*, 2648.
[166] J. Heitz, H. Niino, A. Yabe, *Jpn. J. Appl. Phys.* **1996**, *35*, 4110.
[167] J.-Y. Zhang, I. W. Boyd, H. Esrom, *Surf. Interface Anal.* **1996**, *24*, 718.
[168] J.-Y. Zhang, H. Esrom, U. Kogelschatz, G. Emig, *Appl. Surf. Sci.* **1993**, *69*, 299.
[169] R. Srinivasan, W. J. Leigh, *J. Am. Chem. Soc.* **1982**, *104*, 6784.
[170] R. Srinivasan, *Polymer* **1982**, *23*, 1863.
[171] M. Shirai, T. Yamamoto, M. Tsunooka, *Polym. Degrad. Stab.* **1999**, *63*, 481.
[172] V. M. Graubner, R. Jordan, O. Nuyken, B. Schnyder, T. Lippert, R. Kotz, A. Wokaun, *Macromolecules* **2004**, *37*, 5936.
[173] V. M. Graubner, R. Jordan, O. Nuyken, R. Kotz, B. Schnyder, T. Lippert, A. Wokaun, *Abstr. Am. Chem. Soc.* **2003**, *225*, U703.
[174] B. Schnyder, T. Lippert, R. Kotz, A. Wokaun, V. M. Graubner, O. Nuyken, *Surf. Sci.* **2003**, *532*, 1067.
[175] W. Noll, "*Chemistry and Technology of Silicones*", Academic, New York 1968.
[176] H. Hillborg, U. W. Gedde, *IEEE Trans. Dielectr. Electr. Insul.* **1999**, *6*, 703.
[177] R. Gorur, E. Cherney, J. Burnham, "*Outdoor Insulation*", College of Engineering and Applied Science, Arizona State University, 1998.
[178] B. Campbell, *Dow Corning Corporation Paper* **1996**.
[179] A. Klumpp, H. Sigmund, *Appl. Surf. Sci.* **1989**, *43*, 301.

© 2005 WILEY-VCH Verlag GmbH & Co. KGaA, Weinheim

[180] O. Joubert, G. Hollinger, C. Fiori, R. A. B. Devine, P. Paniez, R. Pantel, *J. Appl. Phys.* **1991**, *69*, 6647.
[181] M. Niwano, K. Kinashi, K. Saito, N. Miyamoto, K. Honma, *J. Electrochem. Soc.* **1994**, *141*, 1556.
[182] A. Barry, *Chem. Tech.* **1983**, *13*, 532.
[183] N. G. Harvey, Y. G. Tropsha, S. L. Burkett, R. P. Clarke, B. S. Wong, *Eur. Pat. Appl.* **1997**, EP 787827, *127*.
[184] Y. G. Tropsha, *Eur. Pat. Appl.* **1997**, EP 787826, *127*.
[185] [185a] "*Handbook of Optical Constants of Solids*", E. D. Palik, Ed., Academic Press, New York 1985; [185b] "*Handbook of Optical Constants of Solids, Vol. 2*", E. D. Palik, Ed., Academic Press, New York 1991.
[186] F. Truica-Marasescu, M. R. Wertheimer, *J. Appl. Polym. Sci.* **2004**, *91*, 3886.
[187] F. E. Truica-Marasescu, P. Jedrzejowski, M. R. Wertheimer, *Plasma Process. Polym.* **2004**, *1*, 153.
[188] T. Shinozuka, M. Shirai, M. Tsunooka, *J. Photopolym. Sci. Technol.* **2000**, *13*, 751.
[189] F. Fuchs, O. Goetzberger, R. Henck, E. Fogarassy, *Appl. Phys. A* **1995**, *60*, 505.

 © 2005 WILEY-VCH Verlag GmbH & Co. KGaA, Weinheim